Frontiers in Nuclear Lattice EFT:
From Ab Initio Nuclear Structure to Reactions
Mar 1-3, 2025, Beijing.

Ab initio calculation of hyper-neutron matter

Hui Tong

☼ *Hui Tong, Serdar Elhatisari, and Ulf-G. Meißner, arXiv.2405.01887(2024)*
☼ *Hui Tong, Serdar Elhatisari, and Ulf-G. Meißner, arXiv.2502.14435(2025)*

Collaborators : Serdar Elhatisari, Ulf-G. Meißner

Contents

- Introduction
- Hyper-Neutron matter
- Summary and Outlook

Neutron stars

- Neutron stars are one of the densest massive objects in the universe.

☼ *A. Sedrakian, et al., PPNP 131, 104041 (2023)*

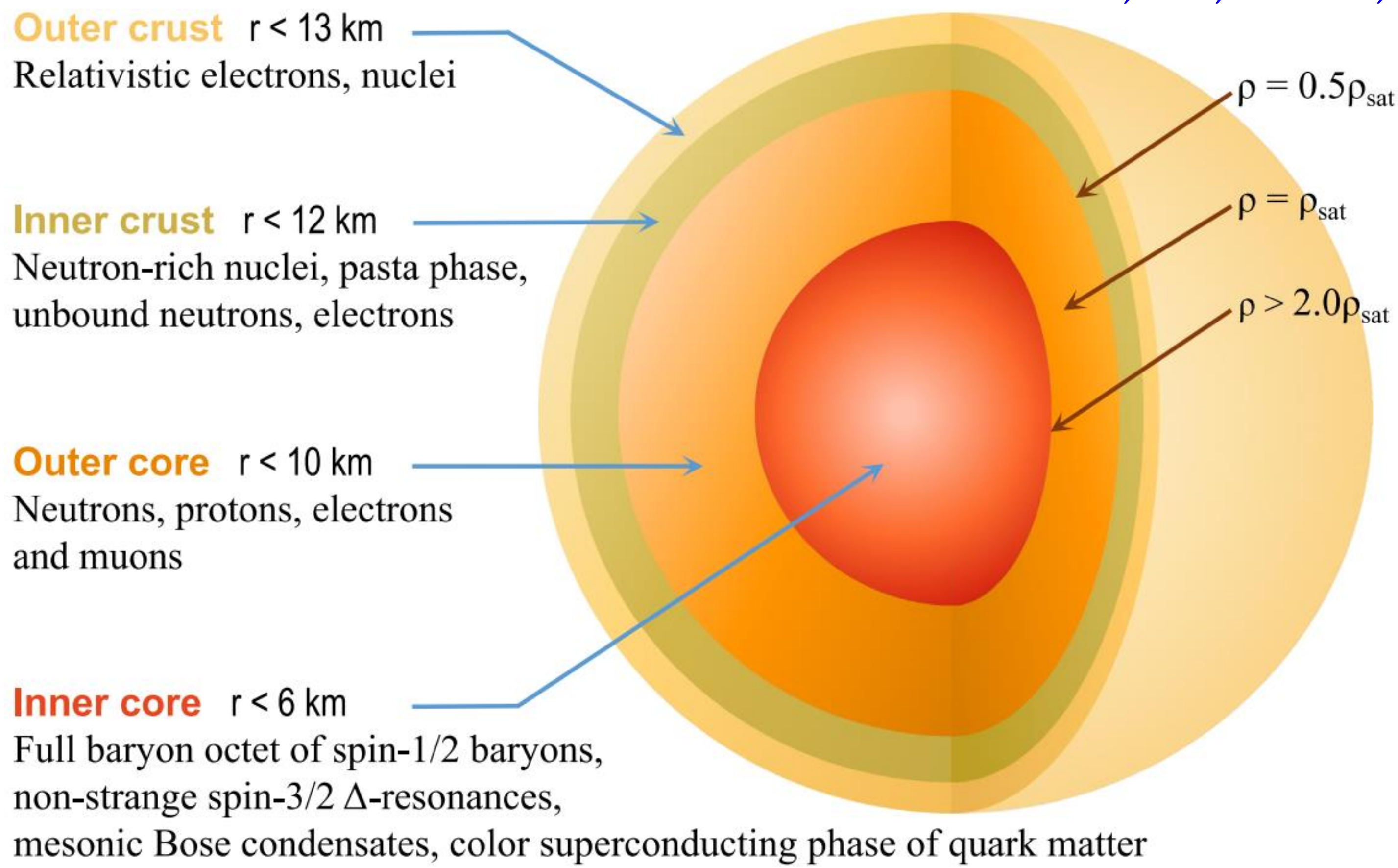

① Usually refer to a star with a mass on the order of 1-2 solar masses, a radius of 10-12 km.

② The central density can reach several times the empirical nuclear matter saturation density ($\rho_{\text{sat}} \approx 0.16\ \text{fm}^{-3}$).

Observations of Neutron stars

- *Mass* measurements

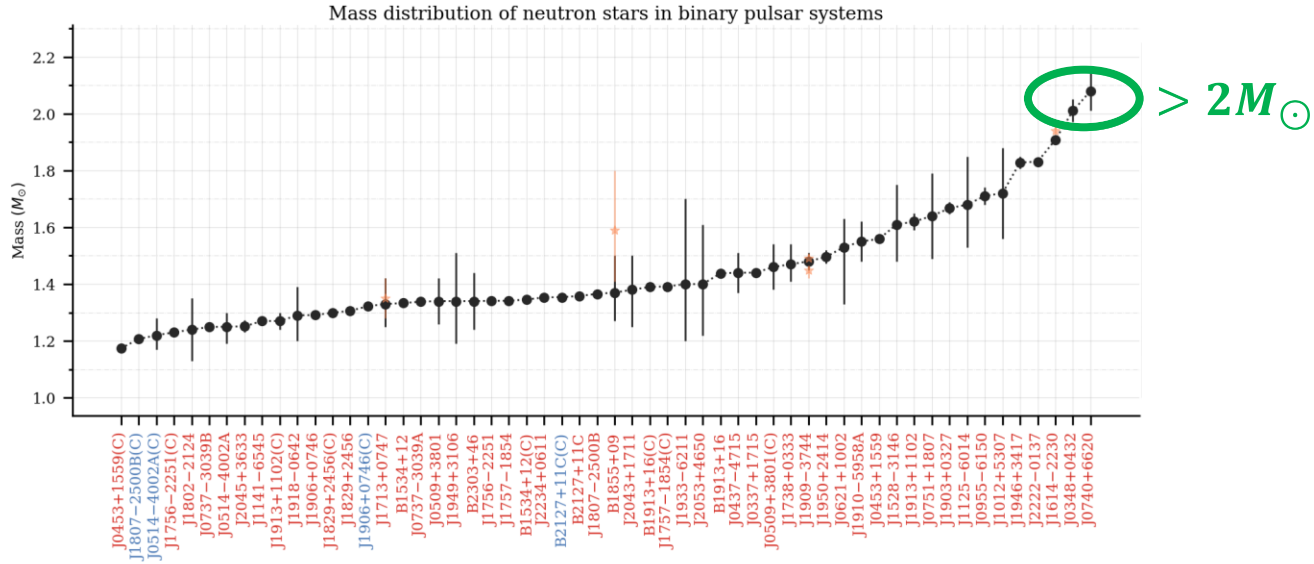

☼ *Figure from Vivek V. Krishnan*

- The *radius* and mass can be measured by the NICER collaboration.

☼ *Raaijmakers, et al., ApJ 887, L22 (2019)*

- The gravitational wave signal provides the astrophysical measurements of *tidal deformabilities*, masses, etc.

☼ *B. P. Abbott, et al., PRL 119, 161101 (2017)*

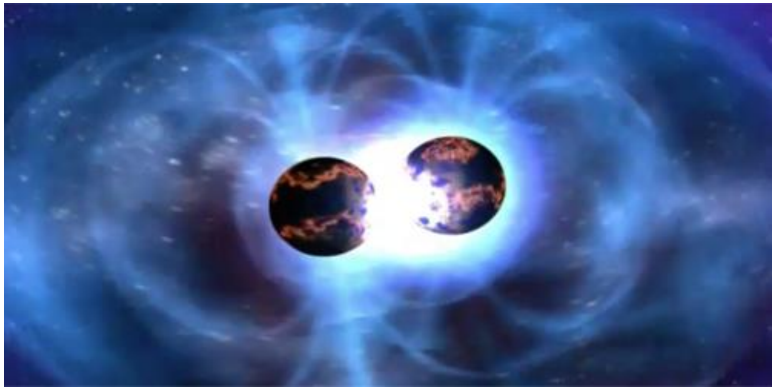

☼ *Figure from NASA/Goddard Space Flight Center*

Hyperon puzzle

- Some of the nuclear many-body approaches, such as Hartree-Fock and Brueckner-Hartree-Fock, predict the appearance of hyperons at a density of $(2-3)\rho_0$, and a softening of the EoS, implying a reduction of the maximum mass.

H. Đapo, et al., PRC 81, 035803 (2010)
H.-J. Schulze and T. Rijken, PRC 84, 035801 (2011)

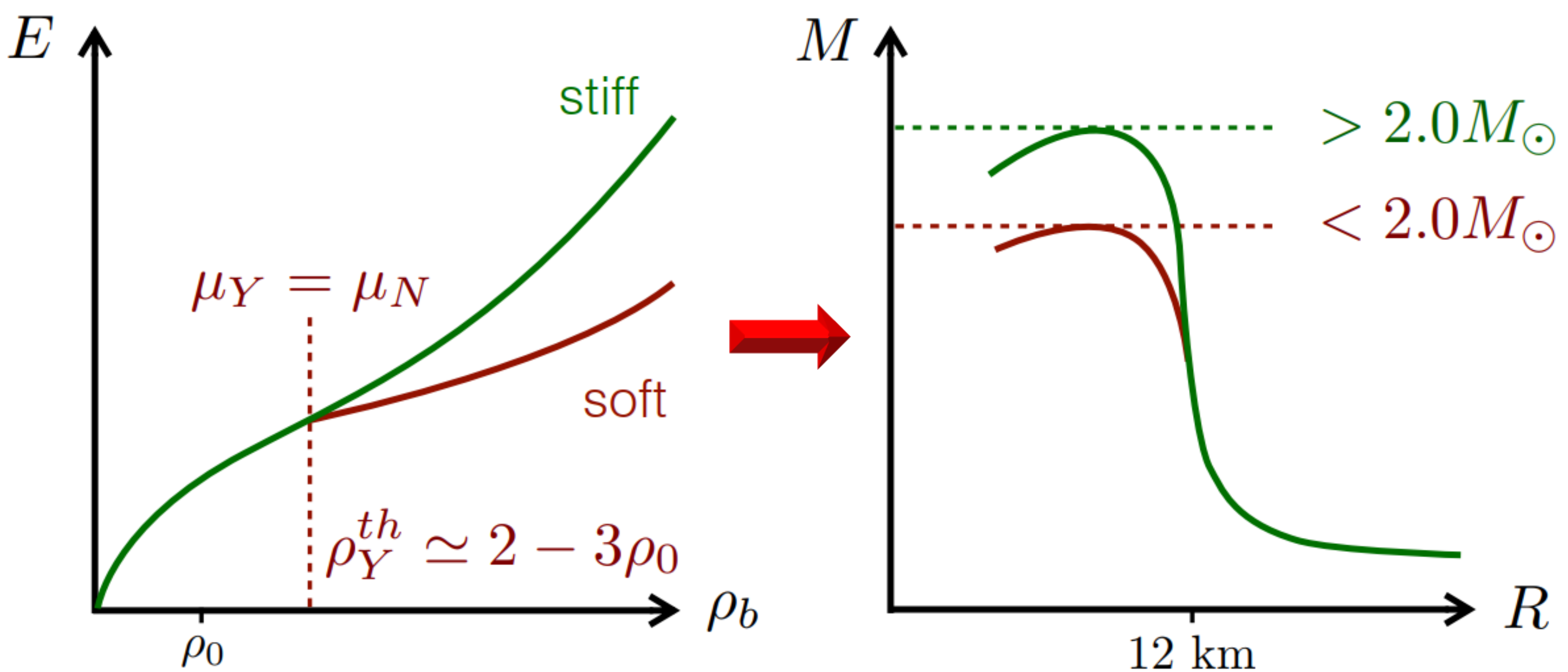

Figure from D. Lonardoni

EoS with Hyperons from AFDMC

- ΛNN(II) can support $2M_{\odot}$, but the onset of Λ is above the maximum density ($0.56\ \mathrm{fm}^{-3}$).

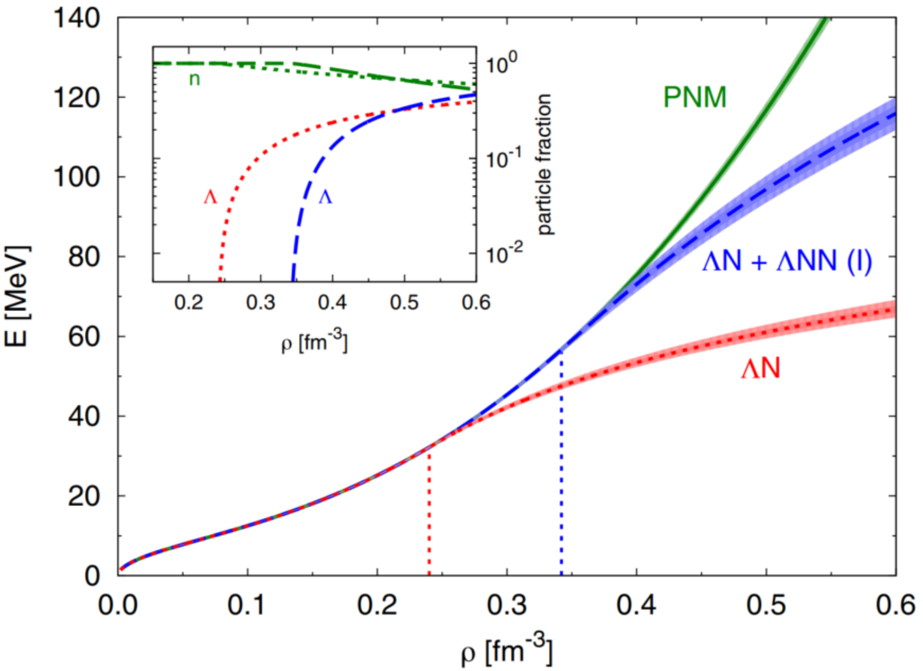

☼ *D. Lonardoni, et al., PRL 114, 092301 (2015)*

① Phenomenological $\Lambda N + \Lambda NN$ potential + Auxiliary field diffusion Monte Carlo, no $\Lambda\Lambda + \Lambda\Lambda N$ potential

② Only some fixed number of neutrons (N_n=66, 54, 38) and hyperons (N_Λ=1, 2, 14) in the simulation box used from AFDMC, the EoS of hyper-neutron matter needs to be parametrized

EoS with Hyperons from AFDMC

- $\Lambda NN(\mathrm{II})$ can support $2M_{\odot}$, but the onset of Λ is above the maximum density ($0.56\ \mathrm{fm}^{-3}$). No Λ present in Neutron Star?

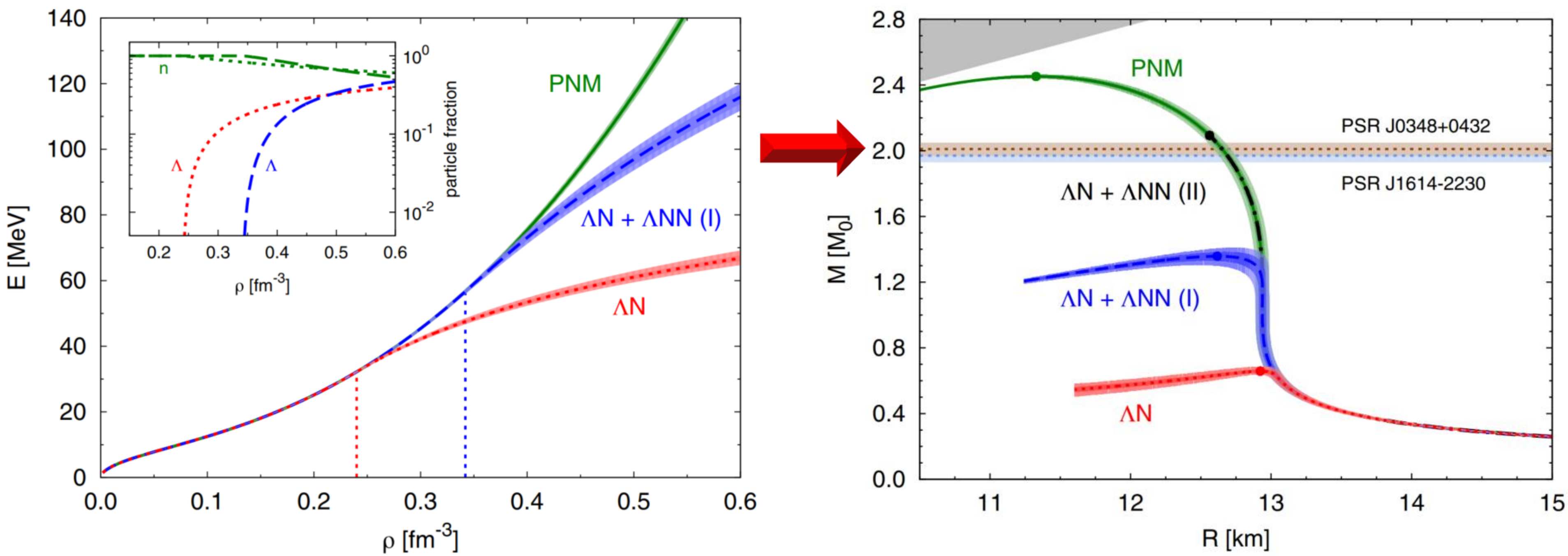

☼ *D. Lonardoni, et al., PRL 114, 092301 (2015)*

① Phenomenological $\Lambda N + \Lambda NN$ potential + Auxiliary field diffusion Monte Carlo, no $\Lambda\Lambda + \Lambda\Lambda N$ potential

② Only some fixed number of neutrons (N_n=66, 54, 38) and hyperons (N_Λ=1, 2, 14) in the simulation box used from AFDMC, the EoS of hyper-neutron matter needs to be parametrized

EoS with Hyperons from AFDMC

- $\Lambda NN(\mathrm{II})$ can support $2M_{\odot}$, but the onset of Λ is above the maximum density ($0.56\ \mathrm{fm}^{-3}$). No Λ present in Neutron Star?

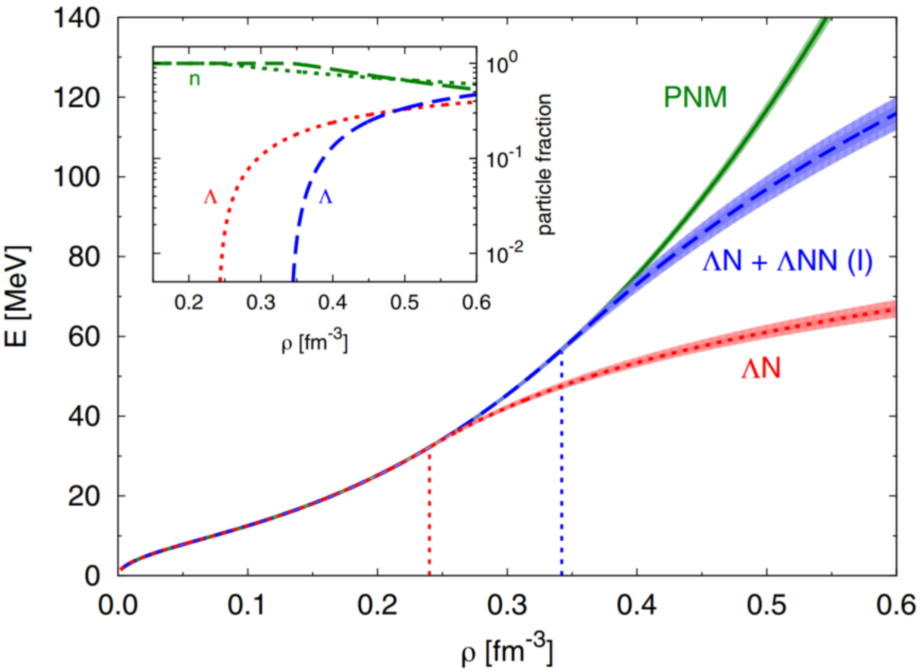

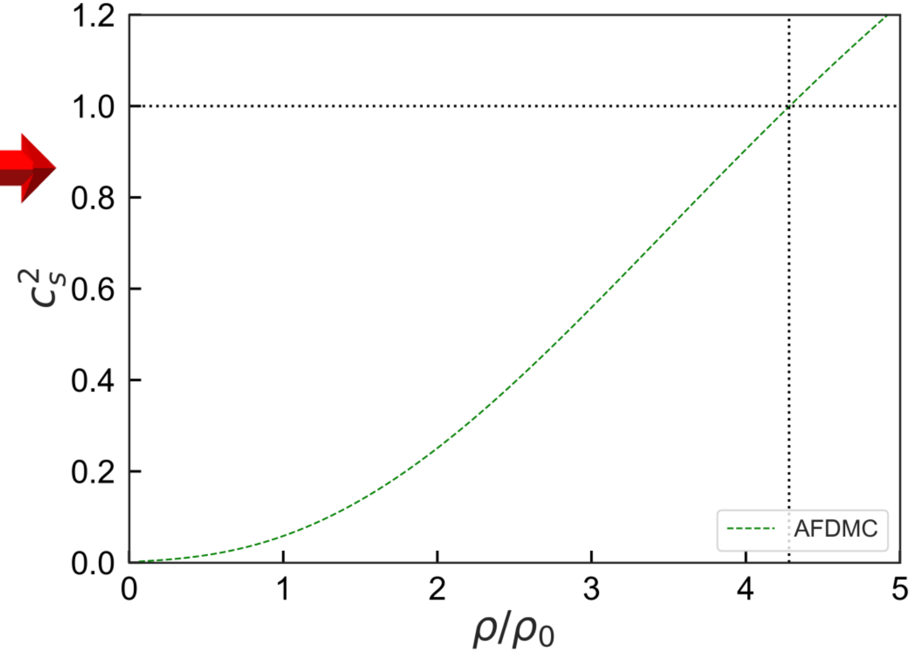

D. Lonardoni, et al., PRL 114, 092301 (2015)

① Phenomenological $\Lambda N + \Lambda NN$ potential + Auxiliary field diffusion Monte Carlo, no $\Lambda\Lambda + \Lambda\Lambda N$ potential

② Only some fixed number of neutrons (N_n=66, 54, 38) and hyperons (N_Λ=1, 2, 14) in the simulation box used from AFDMC, the EoS of hyper-neutron matter needs to be parametrized

EoS with Hyperons from AFDMC

- ΛNN(II) can support $2M_\odot$, but the onset of Λ is above the maximum density ($0.56\ \mathrm{fm}^{-3}$). No Λ present in Neutron Star?

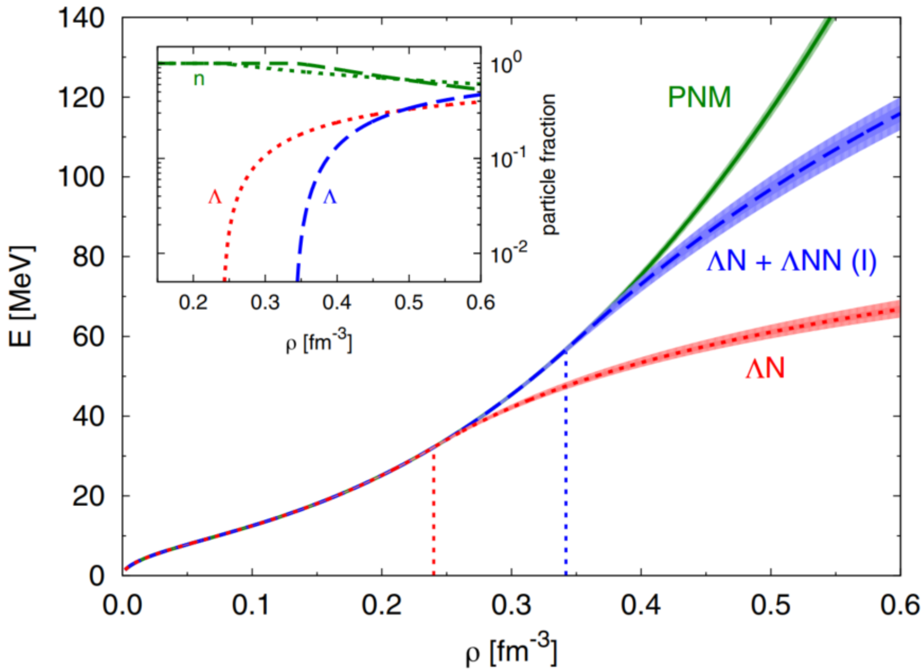

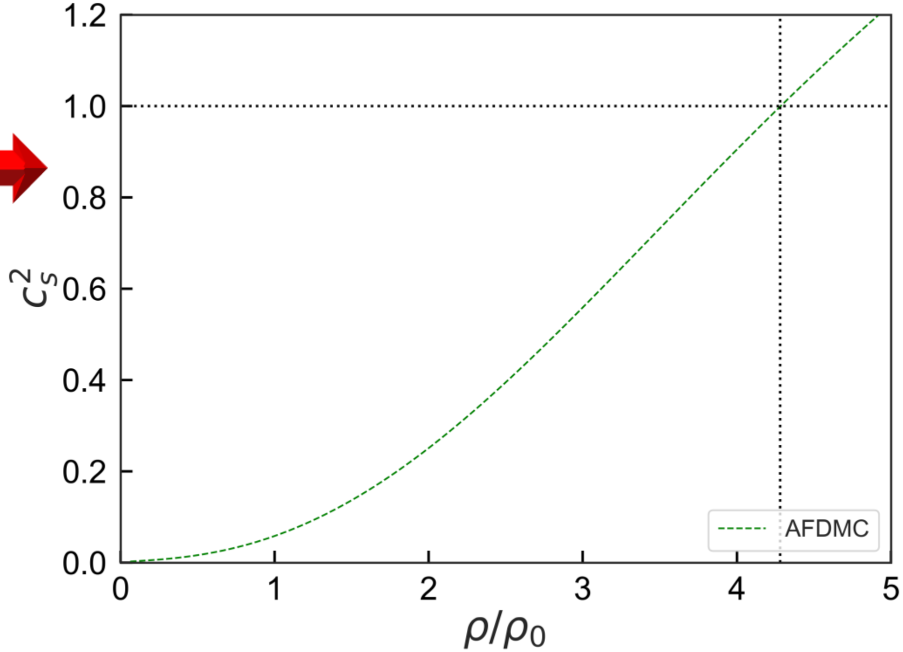

D. Lonardoni, et al., PRL 114, 092301 (2015)

In this work

The hyper-neutron matter and neutron star properties are studied by Nuclear Lattice Effective Field Theory with a novel auxiliary field quantum Monte Carlo algorithm.

Contents

The Hamiltonian for nucleons

- Hamiltonian

$$H = H_{\text{free}} + \frac{c_{NN}}{2} \sum_{\vec{n}} :[\tilde{\rho}(\vec{n})]^2: + \frac{c_{NN}^T}{2} \sum_{I,\vec{n}} :[\tilde{\rho}_I(\vec{n})]^2: + V_{NN}^{\text{GIR}} + V_{\text{Coulomb}} + V_{NNN}$$

the density operator $\tilde{\rho}(\vec{n})$ is defined as

$$\tilde{\rho}(\vec{n}) = \sum_{i,j=0,1} \tilde{a}_{i,j}^{\dagger}(\vec{n})\, \tilde{a}_{i,j}(\vec{n}) + s_{\text{L}} \sum_{|\vec{n}-\vec{n}'|^2=1} \sum_{i,j=0,1} \tilde{a}_{i,j}^{\dagger}(\vec{n}')\, \tilde{a}_{i,j}(\vec{n}')$$

where i is the spin index, j is the isospin index. The smeared annihilation and creation operators are defined as

$$\tilde{a}_{i,j}(\vec{n}) = a_{i,j}(\vec{n}) + s_{\text{NL}} \sum_{|\vec{n}'-\vec{n}|=1} a_{i,j}(\vec{n}')$$

the parameter s_{L} is a local smearing parameter, s_{NL} is a nonlocal smearing parameter. C_{NN} and C_{NN}^T gives the strength of the two-body interaction. V_{NNN} is the three-body interaction.

Phase shift for nucleons

- The C_{NN} couplings are determined by fitting the phase shift.

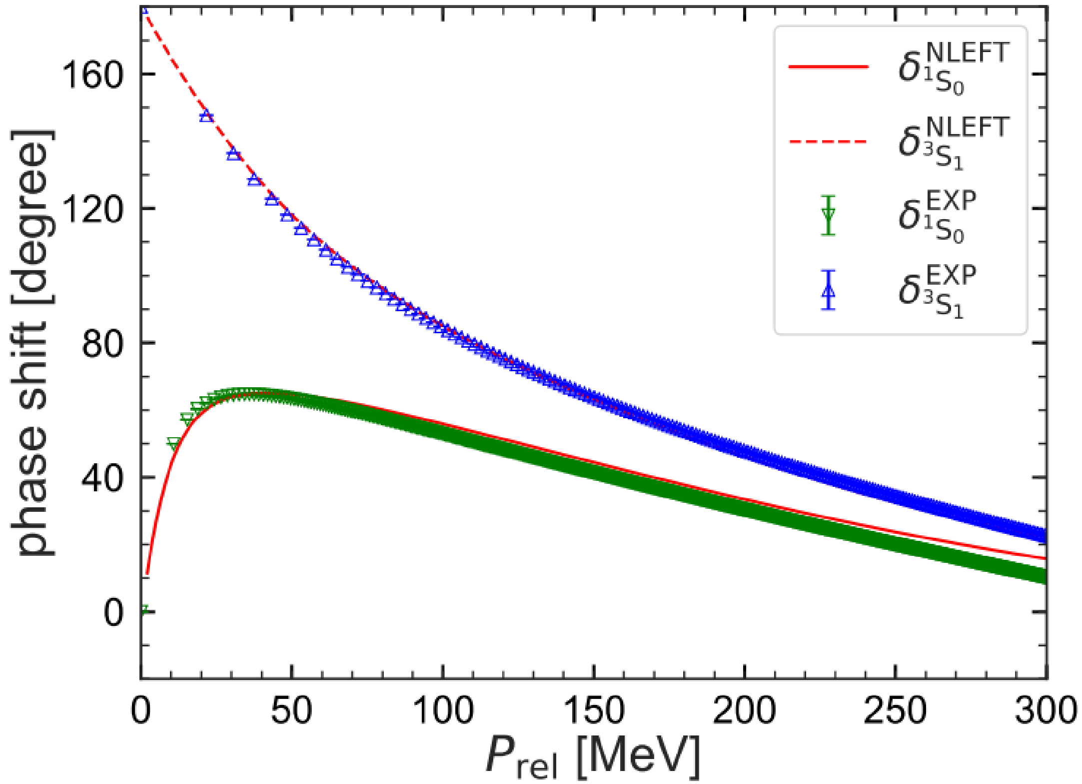

- The Galilean invariance restoration for each channel are obtained by tuning $C_{\mathrm{GIR},i}(i = 0,1,2)$ with the constraint

$$\boxed{C_{\mathrm{GIR},0} + 6C_{\mathrm{GIR},1} + 12C_{\mathrm{GIR},2} = 0}$$

Nuclear Matter and light nuclei

- The couplings for three-body interaction are determined by the empirical value for nuclear matter. As a prediction, the compression modulus $K_\infty = 229.0(3.6)$ MeV.

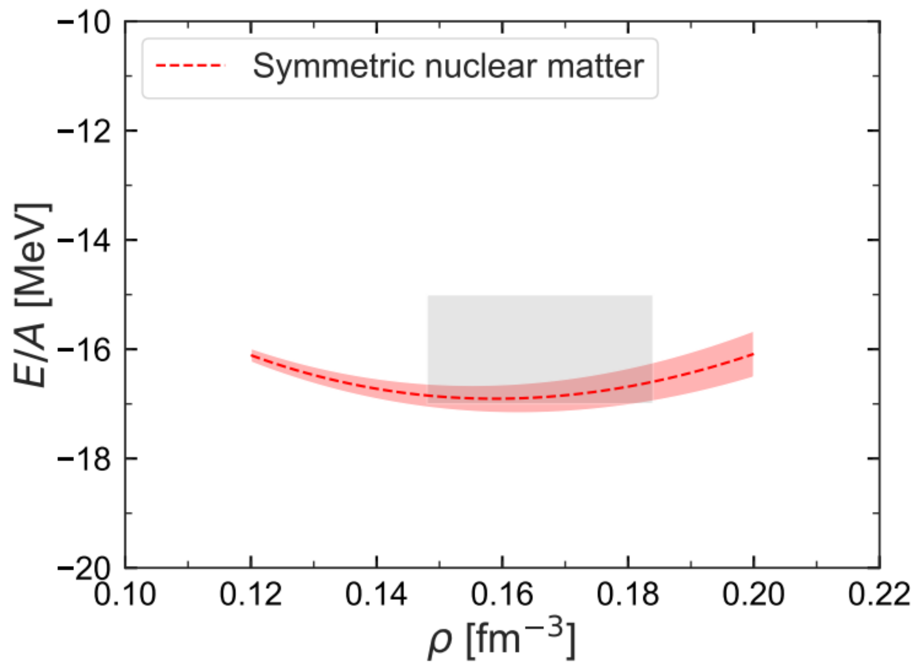

- The ground state energies of several light nuclei (prediction).

Nucleus	NLEFT	Exp.
^{3}H	$-9.21(4)(1)$	-8.48
^{4}He	$-29.38(1)(4)$	-28.3
^{8}Be	$-58.38(3)(7)$	-56.5
^{12}C	$-87.08(12)(11)$	-92.2
^{16}O	$-121.84(28)(52)$	-127.6

Pure Neutron Matter (PNM)

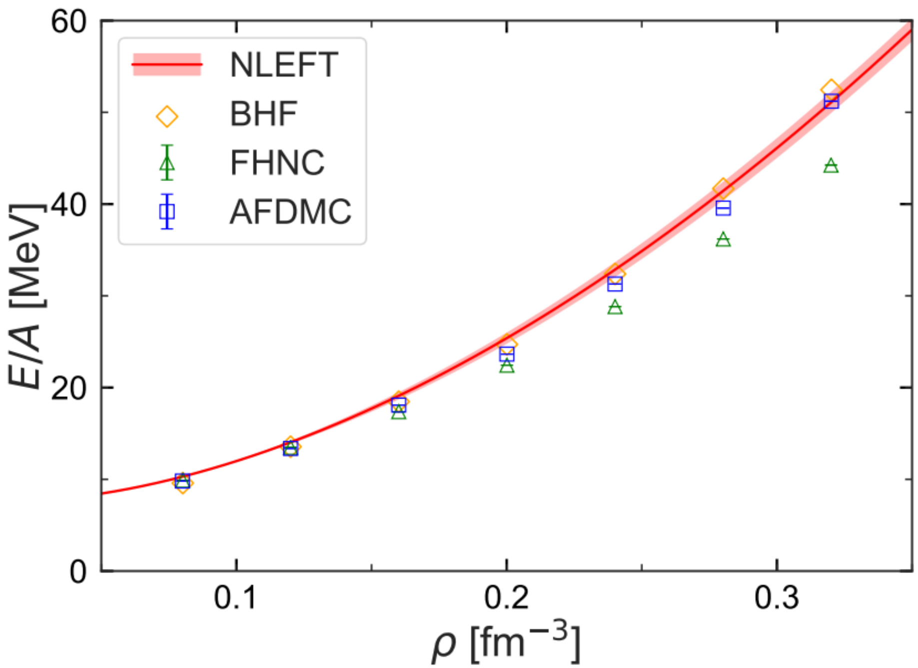

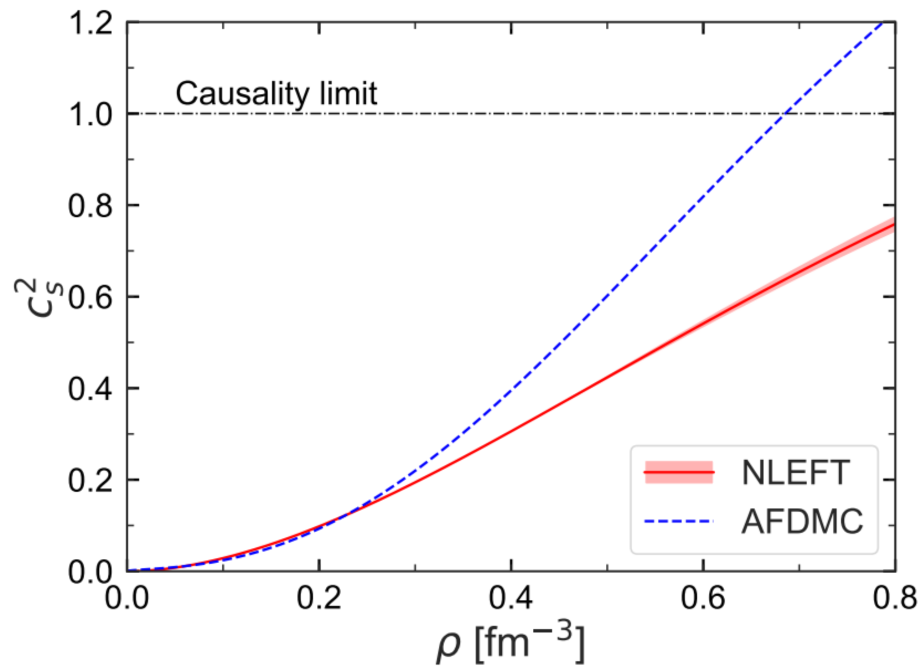

① NLEFT: The calculations are performed for PNM by considering up to 232 neutrons in a box to achieve several times the saturation density

② AFDMC : AV8’+3N interaction inspired by the Urbana IX and the Illinois models

The Hamiltonian for nucleons and hyperons

- For the hyperon-nucleon and hyperon-hyperon interactions, we utilize minimal interactions. The Hamiltonian is defined as,

$$
\begin{aligned}
H = & H_{\text{free}} + \frac{c_{NN}}{2}\sum_{\vec{n}} :\left[\tilde{\rho}(\vec{n})\right]^2: + \frac{c_{NN}^{T}}{2}\sum_{I,\vec{n}} :\left[\tilde{\rho}_I(\vec{n})\right]^2: \\
& + c_{N\Lambda}\sum_{\vec{n}} :\tilde{\rho}(\vec{n})\tilde{\xi}(\vec{n}): + \frac{c_{\Lambda\Lambda}}{2}\sum_{\vec{n}} :\left[\tilde{\xi}(\vec{n})\right]^2: \\
& + V_{NN}^{\text{GIR}} + V_{N\Lambda}^{\text{GIR}} + V_{\Lambda\Lambda}^{\text{GIR}} + V_{\text{Coulomb}} \\
& + V_{NNN} + V_{NN\Lambda} + V_{N\Lambda\Lambda}\,,
\end{aligned}
$$

$C_{N\Lambda}, C_{\Lambda\Lambda}$ give the strength of the two-body interactions. $V_{NN\Lambda}$ and $V_{N\Lambda\Lambda}$ are the three-body interactions. ***The simulation of systems with both neutrons and Λ hyperons can be achieved by using a single auxiliary field.***

Auxiliary Field for Hyper-nuclear Systems

- A discrete auxiliary field formulation for the SU(4) interaction,

$$: \exp\left(-\frac{a_t\, c_{NN}}{2}\,\tilde{\rho}^2\right) := \sum_{k=1}^{3} w_k \;: \exp\left(\sqrt{-a_t\, c_{NN}}\, s_k\, \tilde{\rho}\right) :$$

where a_t is the temporal lattice spacing.

- The two-baryon interactions,

$$V_{2\mathrm{B}} = \frac{c_{NN}}{2}\sum_{\vec{n}} :\, [\tilde{\rho}(\vec{n})]^2 \,: + c_{N\Lambda}\sum_{\vec{n}} :\, \tilde{\rho}(\vec{n})\tilde{\xi}(\vec{n}) \,: + \frac{c_{\Lambda\Lambda}}{2}\sum_{\vec{n}} :\, \left[\tilde{\xi}(\vec{n})\right]^2 :$$

this potential can be rewritten in the following form,

$$V_{2\mathrm{B}} = \frac{c_{NN}}{2}\sum_{\vec{n}} :\, \left[\tilde{\phi}(\vec{n})\right]^2 \,: + \frac{1}{2}\left(c_{\Lambda\Lambda} - \frac{c_{N\Lambda}^2}{c_{NN}}\right)\sum_{\vec{n}} :\, \left[\tilde{\xi}(\vec{n})\right]^2 :$$

where $\tilde{\phi} = \tilde{\rho} + \frac{c_{N\Lambda}}{c_{NN}}\,\tilde{\xi}$, the simulations of systems consisting of both arbitrary number of nucleons and Λs with a single auxiliary field,

$$: \exp\left(-\frac{a_t\, c_{NN}}{2}\,\tilde{\phi}^2\right) := \sum_{k=1}^{3} w_k \;: \exp\left(\sqrt{-a_t\, c_{NN}}\, s_k\, \tilde{\phi}\right) :$$

Scattering data with hyperons

- $C_{N\Lambda}$ is determined by fitting the cross section, and $C_{\Lambda\Lambda}$ by fitting the chiral EFT phase shift.

J. Haidenbauer, Ulf-G. Meißner, and S. Petschauer, Nucl. Phys. A 954, 273 (2016).

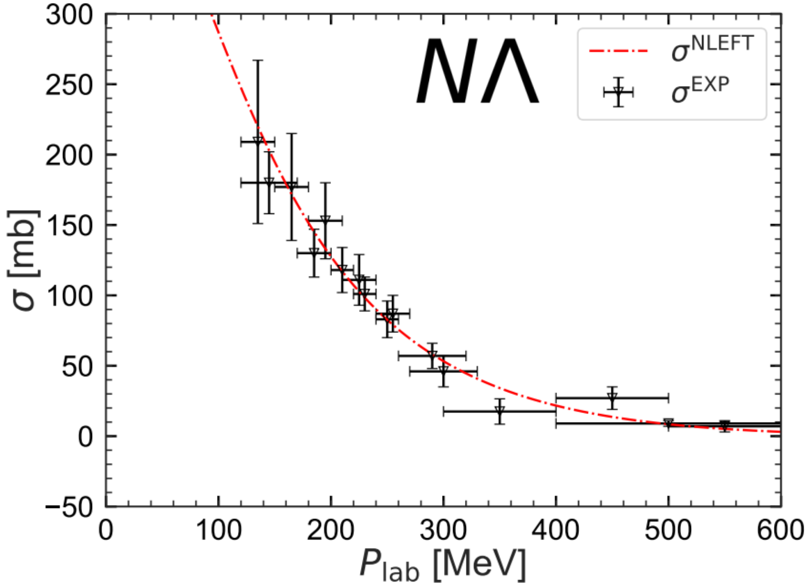

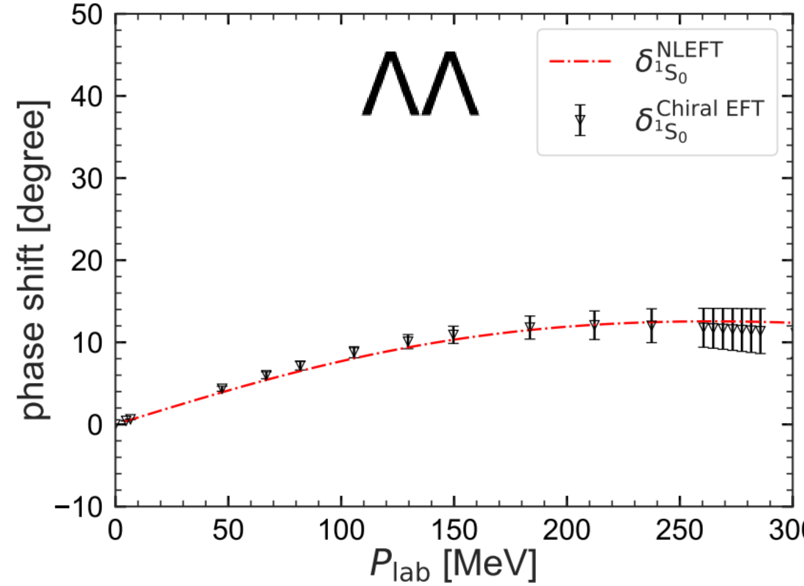

- Three sets of three-body forces are determined by the separation energies for Λ hyper-nuclei. The * marks a prediction.

System	NLEFT			Exp.
	HNM(I)	HNM(II)	HNM(III)	
$^5_\Lambda$He	3.40(1)(1)	3.45(1)(2)	3.46(1)(3)	3.10(3)
$^9_\Lambda$Be	5.72(5)(4)	5.64(5)(3)	5.57(5)(3)	6.61(7)
$^{13}_\Lambda$C	10.54(17)(29)*	10.09(17)(27)*	9.80(17)(26)*	11.80(16)
$^6_{\Lambda\Lambda}$He	6.91(1)(1)	6.91(1)(1)	6.91(1)(1)	6.91(16)

Neutron Star EoS

- The energy density can be obtained as

$$\varepsilon_{\mathrm{HNM}} = \rho[E_{\mathrm{HNM}}(\rho_n, \rho_\Lambda)/N + \frac{\rho_n}{\rho} m_n + \frac{\rho_\Lambda}{\rho} m_\Lambda],$$

the chemical potentials for neutrons and lambdas are evaluated via

$$\mu_n(\rho, x) = \frac{\partial \varepsilon_{\mathrm{HNM}}}{\partial \rho_n}, \mu_\Lambda(\rho, x) = \frac{\partial \varepsilon_{\mathrm{HNM}}}{\partial \rho_\Lambda},$$

the Λ threshold density ρ_Λ^{th} is determined by imposing $\mu_\Lambda = \mu_n$, and the pressure is defined as

$$P(\rho) = \rho^2 \frac{d}{d\rho} \frac{\varepsilon_{\mathrm{HNM}}}{\rho} = \sum_{i=n,\Lambda} \rho_i \mu_i - \varepsilon_{\mathrm{HNM}}.$$

Energy density for different number of hyperons

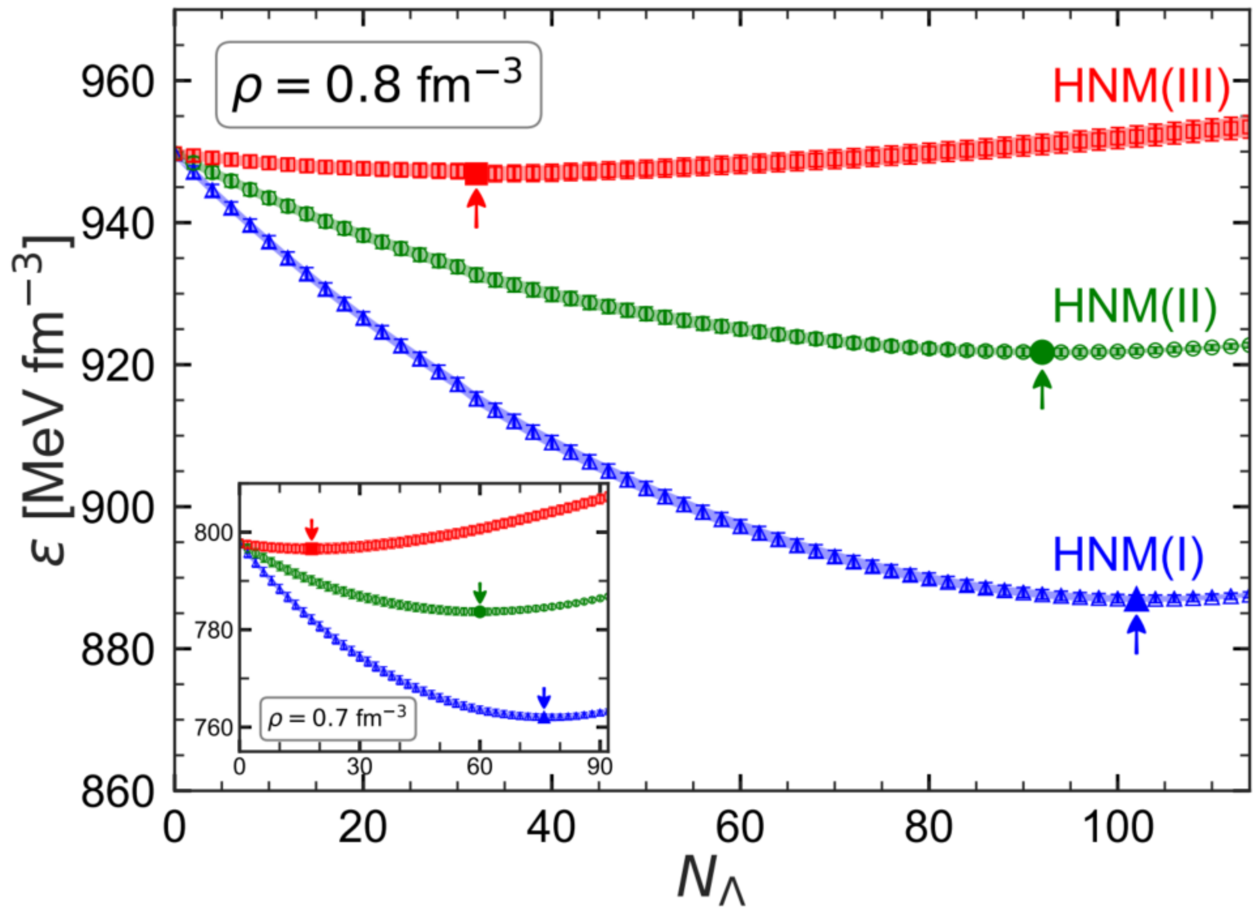

① ***Different number of hyperons can be simulated in our calculations.***

② HNM(I,II,III) have different couplings for $NN\Lambda$ and $N\Lambda\Lambda$ interactions.

③ Only N_n=66,54,38 and N_Λ=1,2,14 are used in AFDMC.

The chemical potential and particle fractions

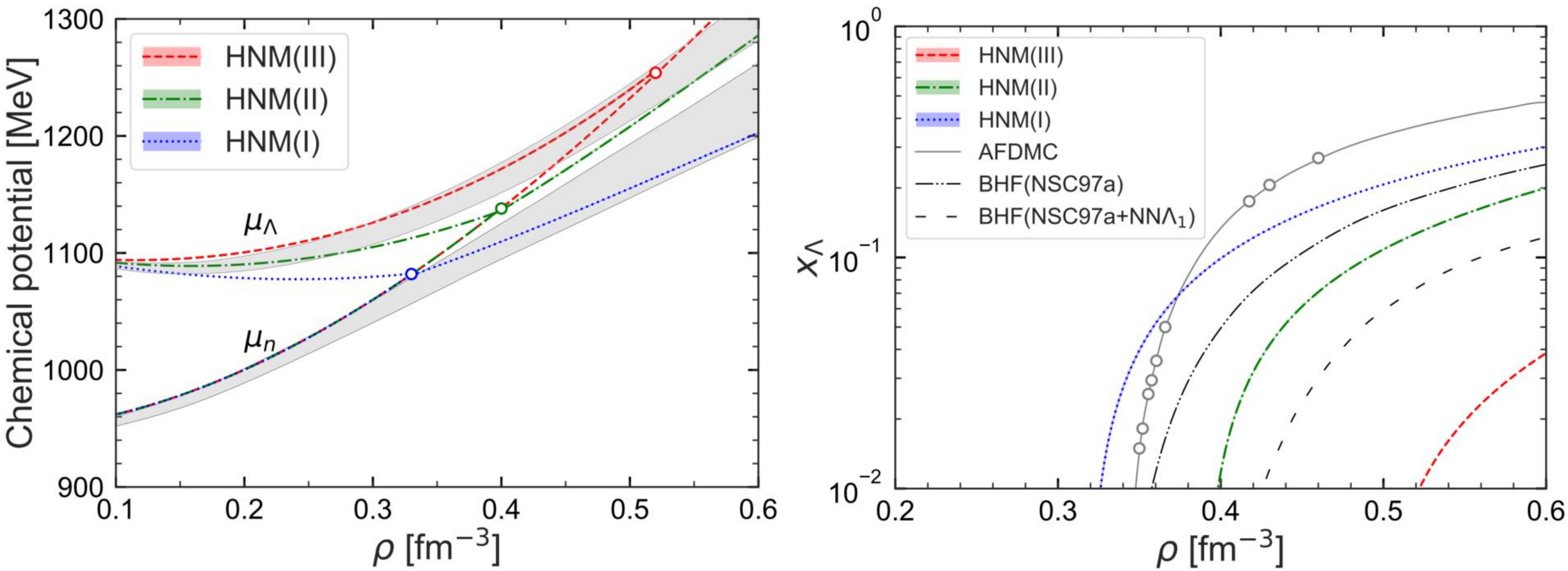

① The Λ threshold densities $\rho_\Lambda^{\rm th}$ are marked by open circles

② The chemical equilibrium conditions, $\mu_n = \mu_\Lambda$, are fulfilled above $\rho_\Lambda^{\rm th}$.

③ The gray shaded area indicates the values by using the chiral SU(3) interactions NLO19 with two and three-body forces ($N\Lambda\ +\ NN\Lambda$)

④ The Λ fraction from the HNM (III) is the smallest one.

Equation of State for hyper-neutron matter

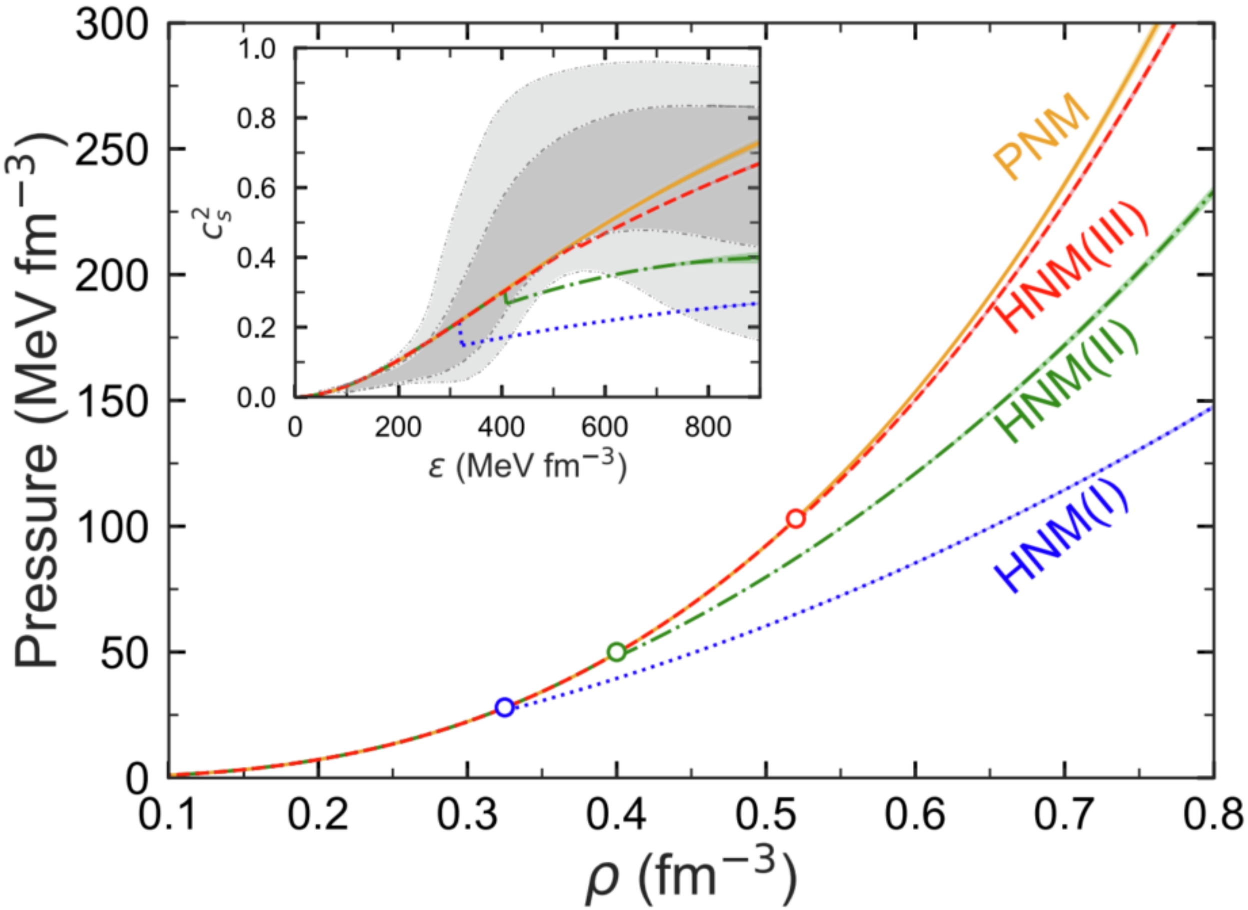

① HNM(I): $\rho_\Lambda^{\mathrm{th}} = 0.325(2)(4)\ \mathrm{fm}^{-3}$ HNM(II): $\rho_\Lambda^{\mathrm{th}} = 0.398(2)(5)\mathrm{fm}^{-3}$

HNM(III): $\rho_\Lambda^{\mathrm{th}} = 0.520(2)(6)\ \mathrm{fm}^{-3}$

② The gray shaded regions are the inference of the speed of sound in view of the recent observational data

☼ L. Brandes, W. Weise, and N. Kaiser, Phys. Rev. D 108, 094014 (2023)

Neutron Star properties

Tolman-Oppenheimer-Volkoff (TOV) equations

☼ *R. C. Tolman, Phys. Rev. 55, 364 (1939)* ☼ *J. R. Oppenheimer and G. M. Volkoff, Phys. Rev. 55, 374 (1939)*

$$\frac{dP(r)}{dr} = -\frac{[P(r)+\varepsilon(r)][M(r)+4\pi r^3 P(r)]}{r[r-2M(r)]},$$

$$\frac{dM(r)}{dr} = 4\pi r^2 \varepsilon(r),$$

where $P(r)$ is the pressure, and $M(r)$ is the total star mass.

Neutron star tidal deformability Λ

☼ *E. E. Flanagan and T. Hinderer, PRD 77, 021502 (2008)* ☼ *T. Hinderer, ApJ 677, 1216 (2008)*

$$\Lambda = \frac{2}{3} k_2 \left(\frac{R}{M}\right)^5,$$

where k_2 is the second Love number

$$\begin{aligned} k_2 = {} & \frac{1}{20}\left(\frac{2M}{R}\right)^5 \left(1-\frac{2M}{R}\right)^2 \left[2 - y_R + (y_R - 1)\frac{2M}{R}\right] \times \left\{\frac{2M}{R}\left(6 - 3y_R + \frac{3M}{R}(5y_R - 8)\right.\right. \\ & \left.\left. + \frac{1}{4}\left(\frac{2M}{R}\right)^2 \left[26 - 22y_R + \frac{2M}{R}(3y_R - 2) + \left(\frac{2M}{R}\right)^2 (1 + y_R)\right]\right) + 3\left(1-\frac{2M}{R}\right)^2 \right. \\ & \left. \times \left[2 - y_R + (y_R - 1)\frac{2M}{R}\right] \log\left(1 - \frac{2M}{R}\right)\right\}^{-1}. \end{aligned}$$

The moment of inertia

- In the slow-rotation approximation, the moment of inertia is

F. J. Fattoyev and J. Piekarewicz, Phys. Rev. C 82, 025810 (2010)

$$I = \frac{8\pi}{3}\int_0^R r^4 e^{-\nu(r)}\frac{\bar{\omega}(r)}{\Omega}\frac{\varepsilon(r)+P(r)}{\sqrt{1-2M(r)/r}}dr$$

The quantity $\nu(r)$ is a radially dependent metric function is defined as

$$\nu(r) = \frac{1}{2}\ln\left(1-\frac{2M}{R}\right) - \int_r^R \frac{M(x)+4\pi x^3 P(x)}{x^2[1-2M(x)/x]}dx$$

The frame-dragging angular velocity $\bar{\omega}$ is usually obtained by the dimensionless relative frequency $\tilde{\omega} \equiv \bar{\omega}/\Omega$, which satisfies

$$\frac{d}{dr}\left[r^4 j(r)\frac{d\tilde{\omega}(r)}{dr}\right] + 4r^3\frac{dj(r)}{dr}\tilde{\omega}(r) = 0$$

where

$$j(r) = e^{-\nu(r)}\sqrt{1-2M(r)/r}$$

Neutron star Mass and radius

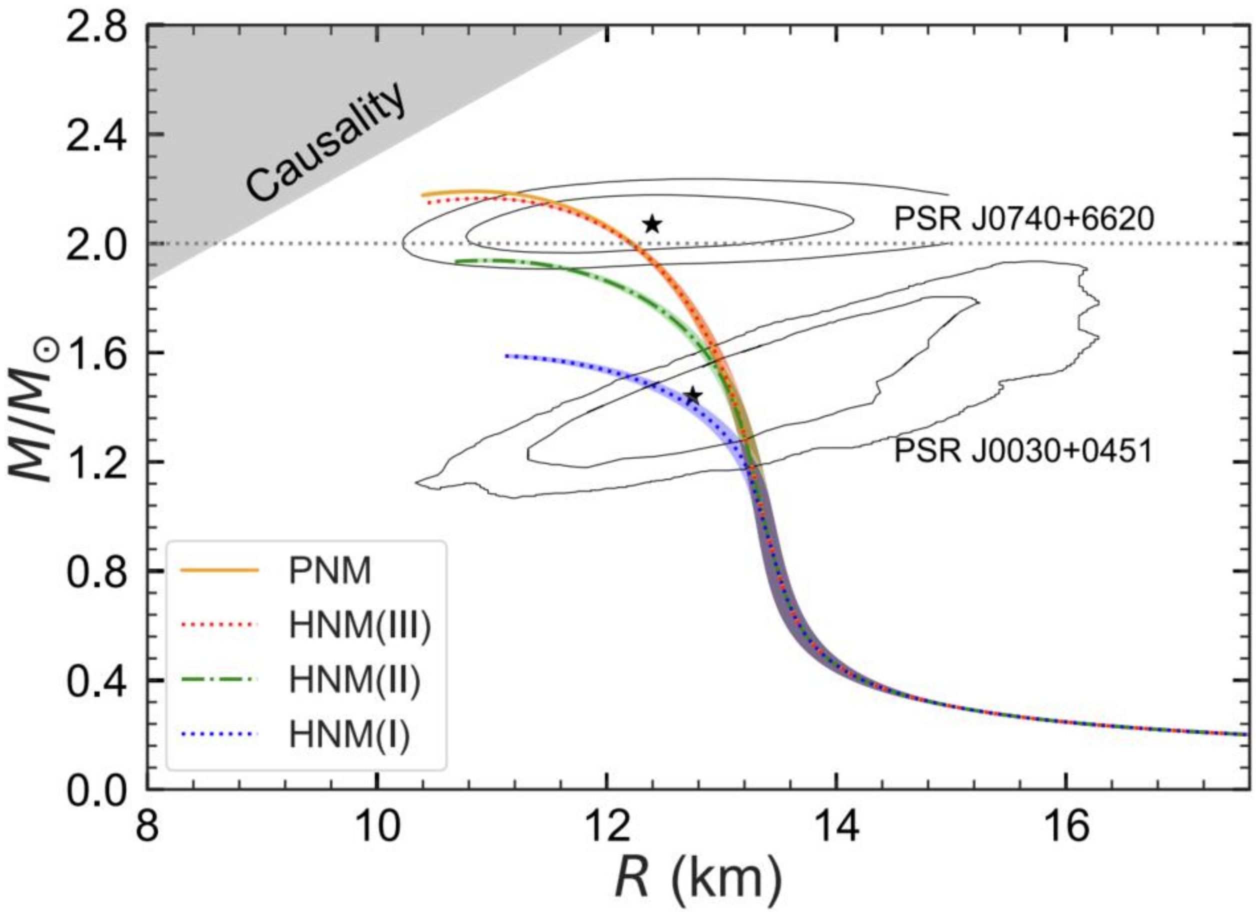

① HNM(I): $M_{\max}$=1.59(1)(1)$M_{\odot}$ HNM(II): $M_{\max}$=1.94(1)(1)$M_{\odot}$

HNM(III): $M_{\max}$=2.17(1)(2)$M_{\odot}$

② PSR J0030+0451 and J0740+6620 : pulsar observed by the NICER.

Neutron star tidal deformability

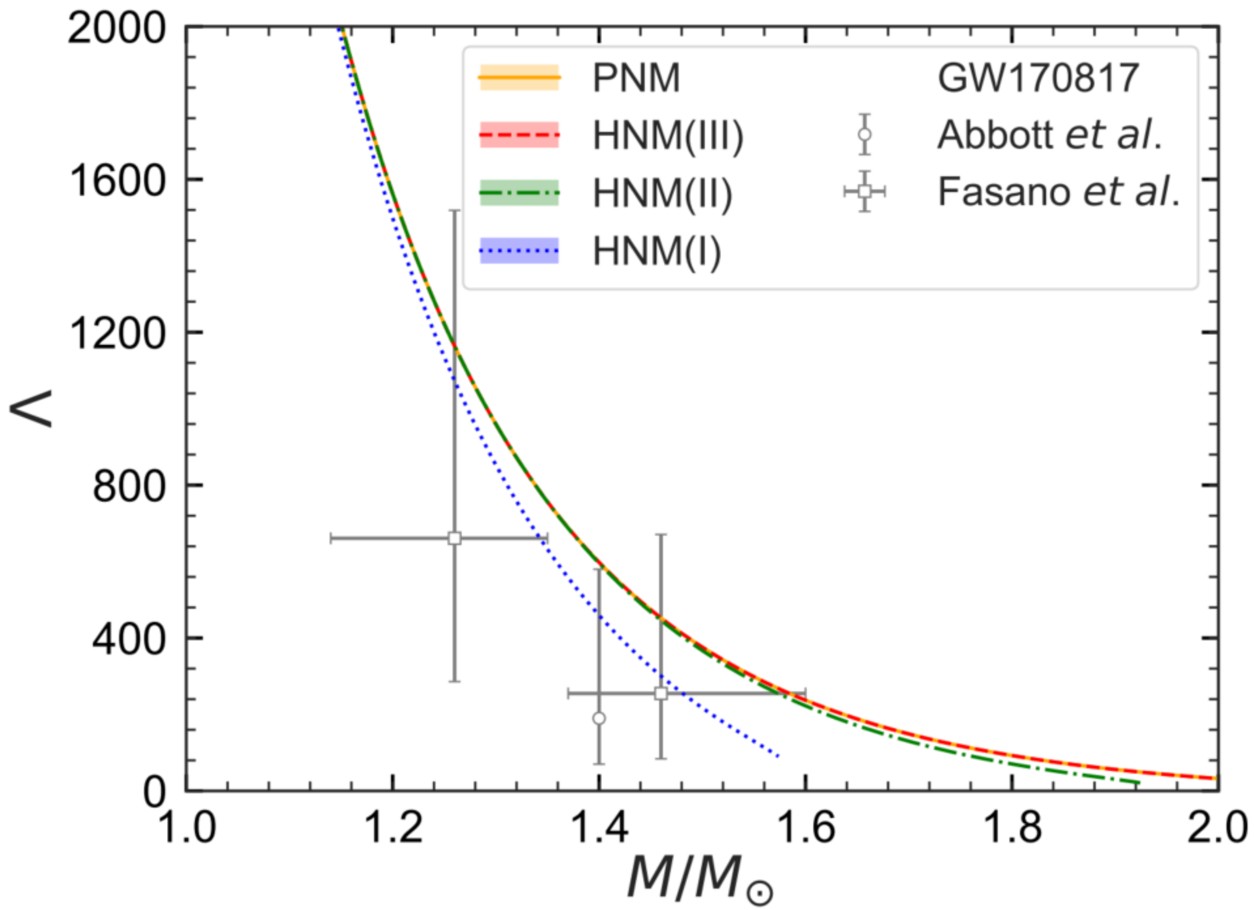

① The neutron star tidal deformabilities Λ are consistent with astrophysical observations of GW170817

☼ *B. P. Abbott, et al., PRL 121, 161101 (2018)*

☼ *M. Fasano, et al., PRL 123, 141101 (2019)*

Universal relations I-Love-Q

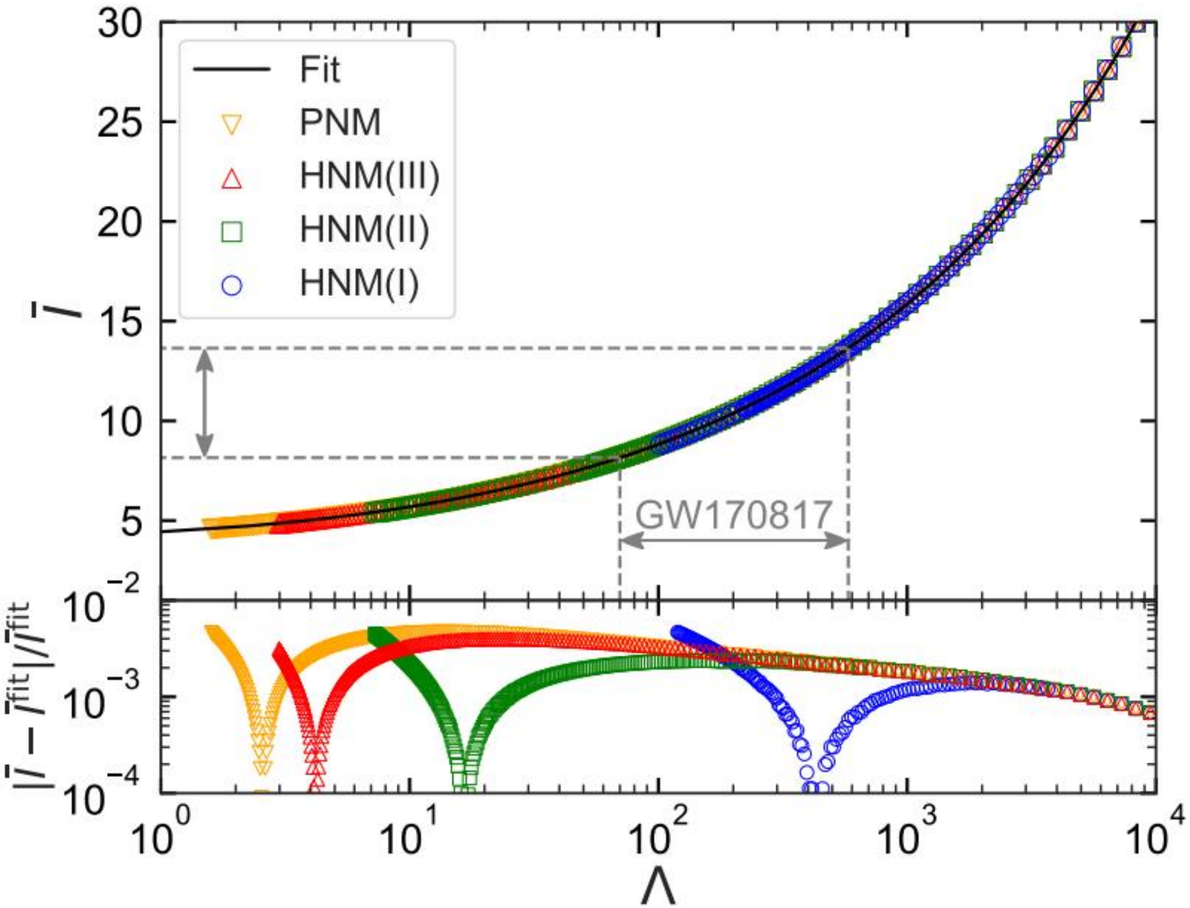

① $\bar{I}$ is the dimensionless quantities for the moment of inertia, 8.2<$\bar{I}$<13.7

② Fitting function

K. Yagi and N. Yunes, Science 341, 365 (2013)

$$\ln y_i = a_i + b_i \ln x_i + c_i (\ln x_i)^2 + d_i (\ln x_i)^3 + e_i (\ln x_i)^4$$

Rotating Neutron Star

- Rotation causes an NS to deform into an oblate spheroid, resulting in a larger equatorial radius and an increased gravitational mass compared to a non-rotating NS, which is related to an increase of the centrifugal force.

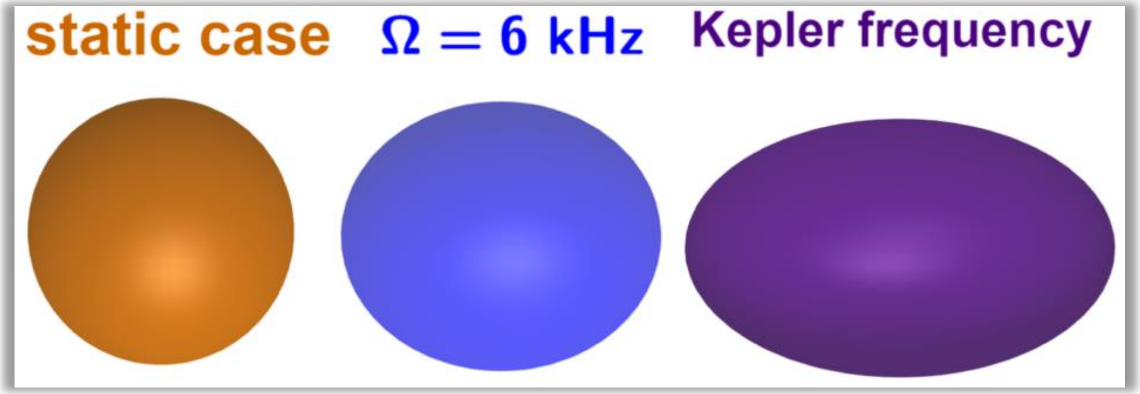

☼ *C. Gartlein, arXiv:2412.07758 (2024)*

The rapidly rotating neutron star can be described by the energy-momentum tensor:

$$\boxed{T^{\mu\nu} = (\varepsilon + P)u^\mu u^\nu - g^{\mu\nu} P,}$$

where u^μ is the fluid's four-velocity.

Rotating Neutron Star Properties

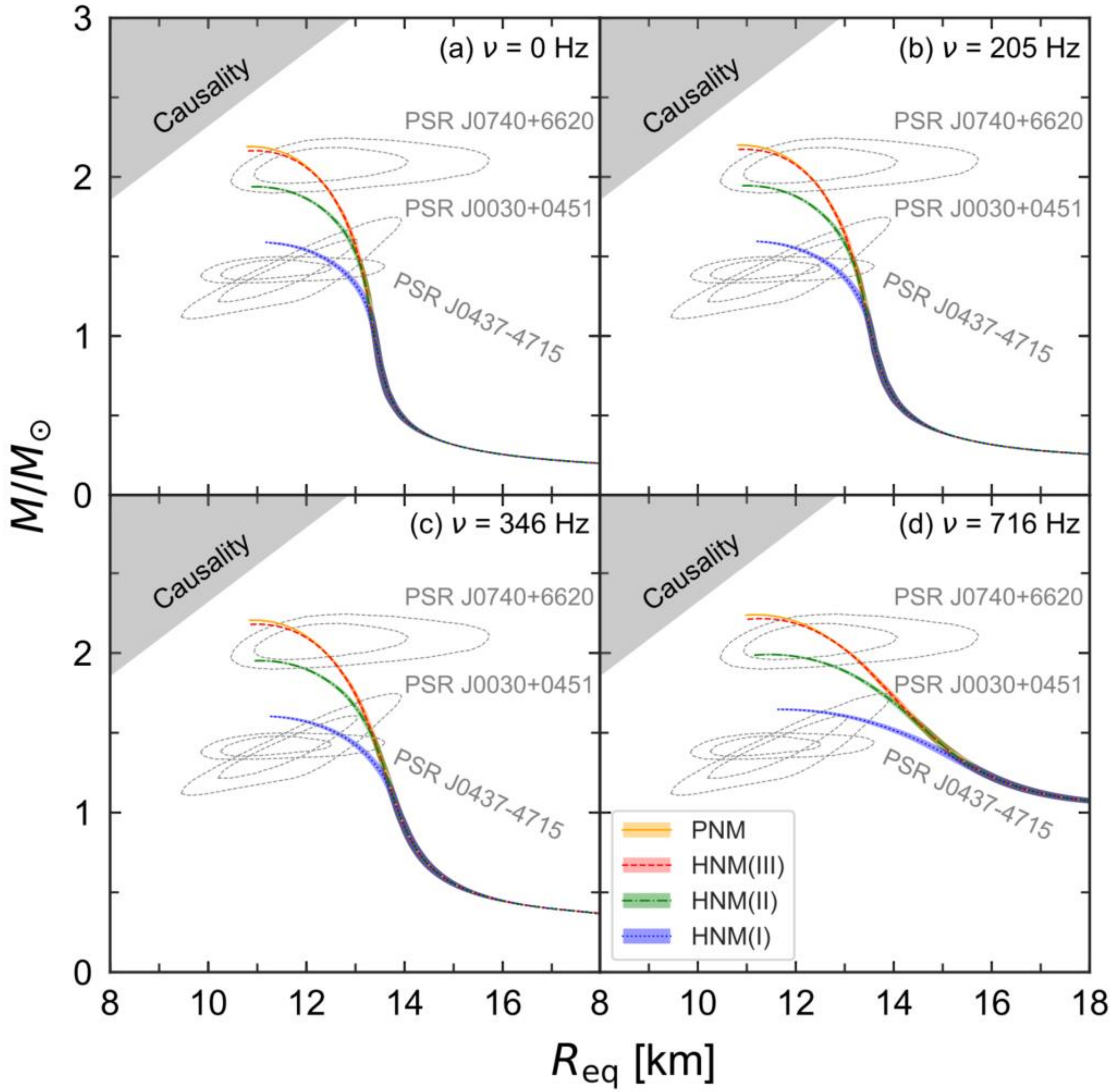

① Four constant spin frequencies ν = 0, 205, 346, 716 Hz are shown

② The impact of rotational dynamics on the maximum mass is small

Hyper β-stable nuclear matter

- The equilibrium conditions and the charge neutrality condition,

$$\mu_n - \mu_p = \mu_e, \quad \mu_e = \mu_\mu, \quad \mu_n = \mu_\Lambda, \quad \rho_p = \rho_e + \rho_\mu.$$

Incorporating protons significantly increases the computational. For example, at $\rho = 0.5\ \mathrm{fm}^{-3}$ (the total number of baryons are 142),

Hyper-neutron matter	Hyper β-stable nuclear matter
108 jobs	1620 jobs

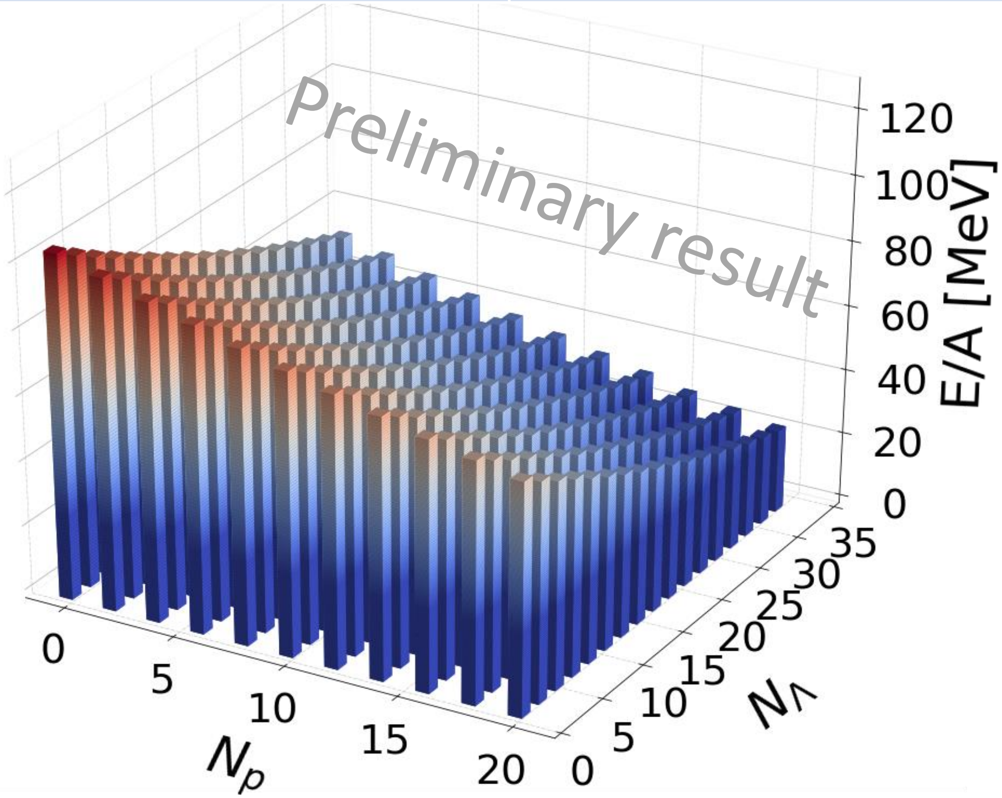

EoS for hyper β-stable nuclear matter

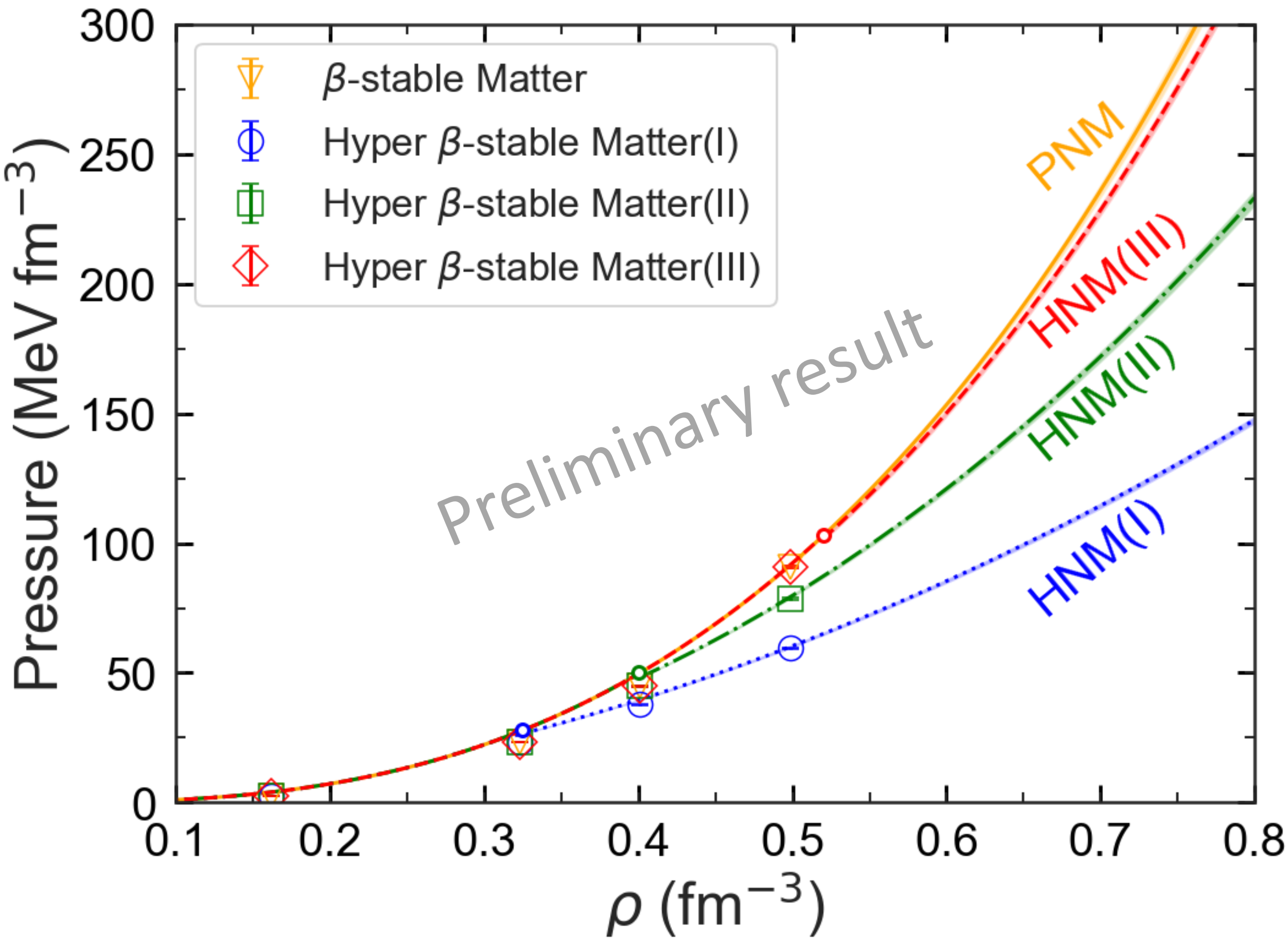

① The presence of protons slightly softens the HNM EoS, and the proton fractions depend on both the symmetry energy and the density.

Contents

- Introduction
- Hyper-Neutron matter
- Summary and Outlook

Summary and Outlook

① A novel auxiliary field quantum Monte Carlo algorithm is introduced, allowing us to simulate for different number of hyperons and neutrons.
② For the first time in *ab initio* calculations, not only include $N\Lambda$ two-body and $NN\Lambda$ three-body forces, but also $\Lambda\Lambda$ and $N\Lambda\Lambda$ interactions are involved.
③ Both the static and rotating neutron star properties are studied.

① Include protons in our simulations. (In progress)
② Include other hyperons in our simulations.
③ Use the recently developed hi-fidelity chiral interactions at N3LO.

Thanks for your attention !

Appendix

EOS from different information channels

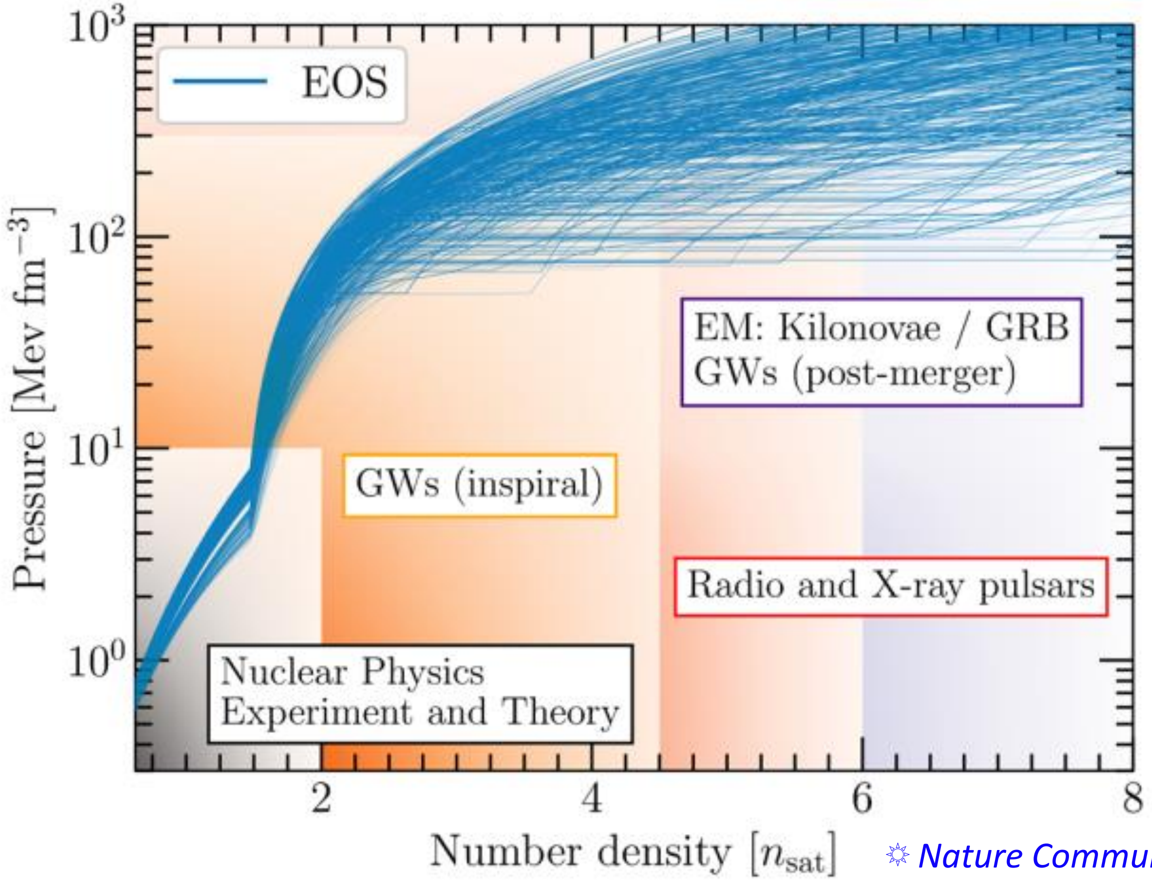

☼ *Nature Communications 14, 8352 (2023)*

Fig. 1 | Overview of constraints on the EOS from different information channels. We show a set of possible EOSs (blue lines) that are constrained up to $1.5n_{sat}$ by Quantum Monte Carlo calculations using chiral EFT interactions[80] and extended to higher densities using a speed of sound model[149]. Different regions of the EOS can then be constrained by using different astrophysical messengers, indicated by rectangulars: GWs from inspirals of NS mergers, data from radio and X-ray pulsars, and EM signals associated with NS mergers. Note that the boundaries are not strict but depend on the EOS and properties of the studied system.

Symmetry energy and EoS

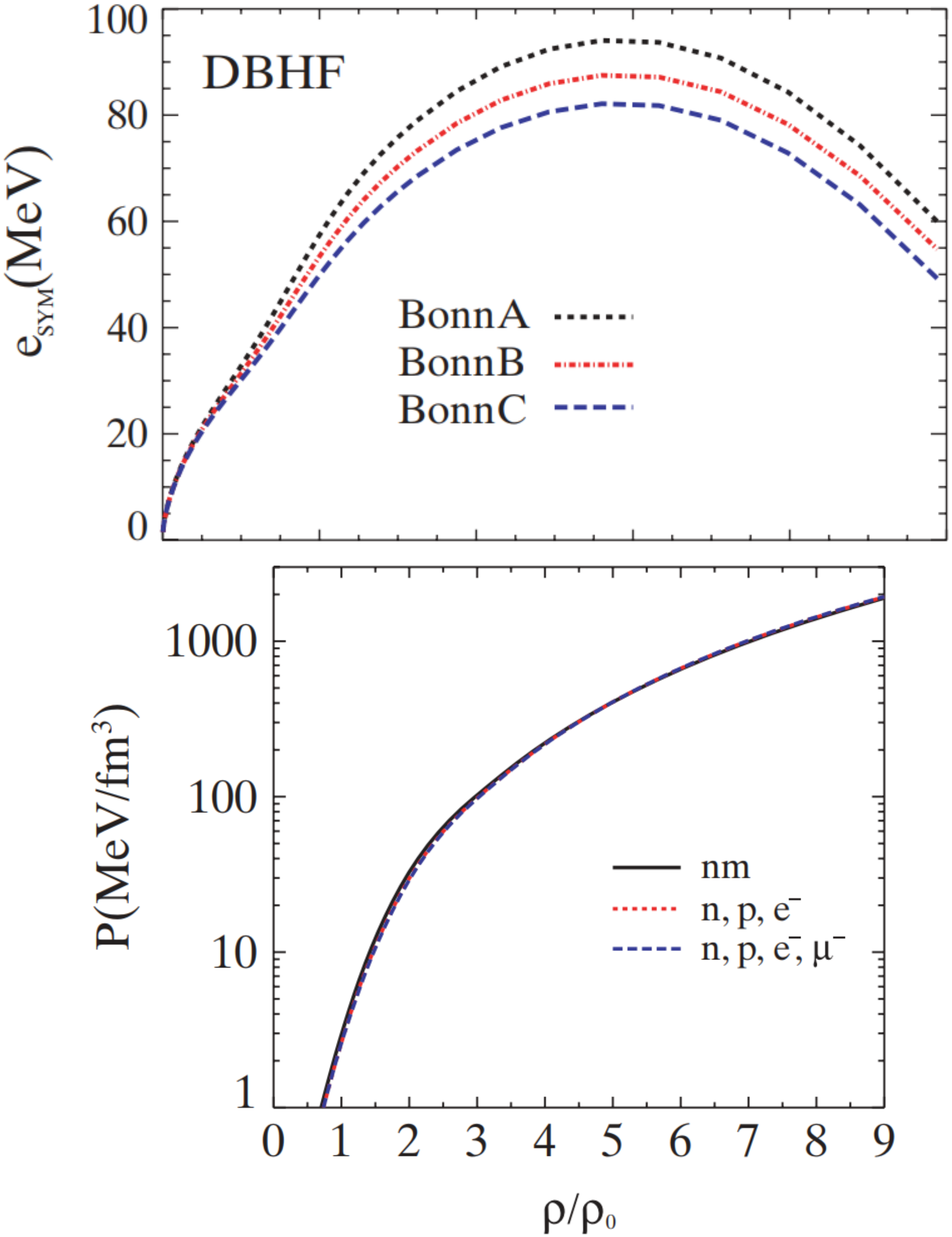

☼ *Physical Review C 74, 025808 (2006)*

I-Love-Q (II)

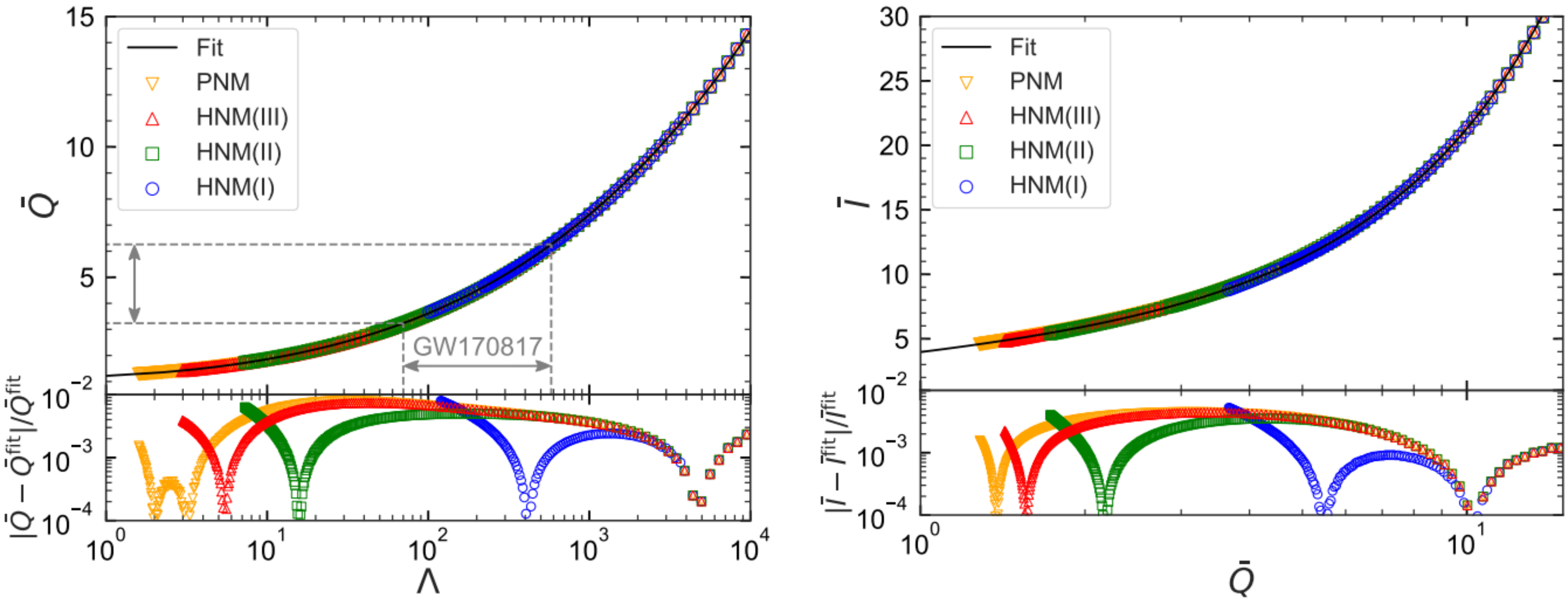

TABLE III. Numerical coefficients for the fit formula of the I-Love, I-Q, and Q-Love relations.

y_i	x_i	a_i	b_i	c_i	d_i	e_i
$\bar{I}$	Λ	1.49093×10^{0}	5.93880×10^{-2}	2.24914×10^{-2}	-6.93727×10^{-4}	7.78146×10^{-6}
$\bar{Q}$	Λ	1.97175×10^{-1}	9.19620×10^{-2}	4.93555×10^{-2}	-4.56214×10^{-3}	1.39647×10^{-4}
$\bar{I}$	$\bar{Q}$	1.40269×10^{0}	5.25610×10^{-1}	4.07856×10^{-2}	1.85656×10^{-2}	1.00574×10^{-4}

J. J. Li, A. Sedrakian, and F. Weber, Phys. Rev. C 108, 025810 (2023).

Finite volume

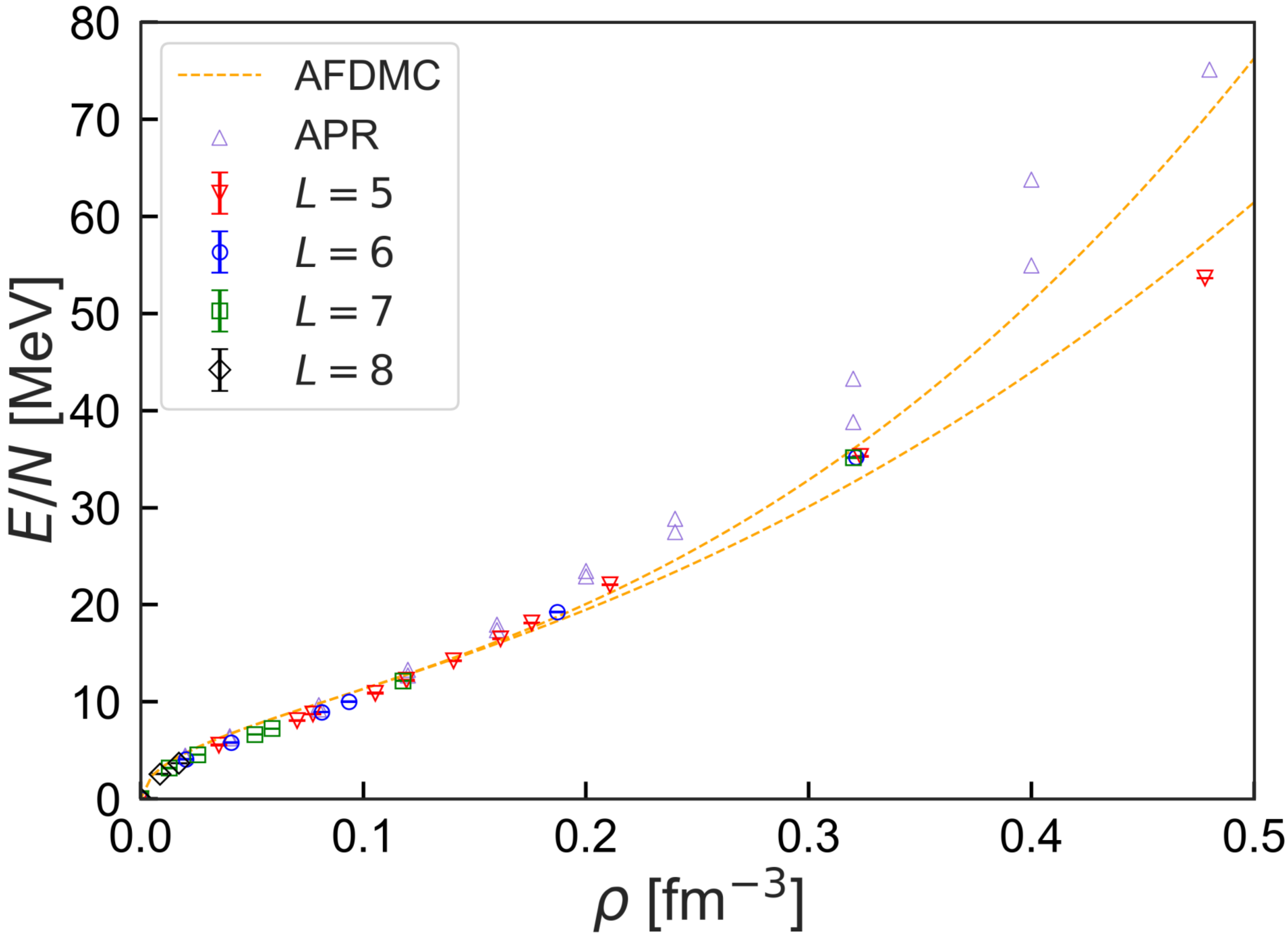

Gerstung et al's work

Next, we compare our work with the one of Gerstung et al. [17]. For the ΛN interaction, they consider two next-to-leading order chiral EFT representations, called NLO13 [95] and NLO19 [96]. For the three-body forces, they use the leading ΛNN representation based on chiral EFT (contact terms, one-pion and two-pion exchanges) with the inclusion of the $\Lambda NN \leftrightarrow \Sigma NN$ transition [97] in an effective density-dependent two-body approximation [98]. The pertinent LECs are given in terms of decuplet resonance saturation and leave one with two B^*BBB couplings, where B denotes the baryon octet and B^* the decuplet. If one only considers the ΛNN force as we do, these two LECs appear in the combination $H' = H_1 + H_2$. No $\Lambda\Lambda N$ force was considered in [17]. The two LECs H_1, H_2 where constrained in[17] so that the Λ single-particle potential in infinite matter is $U_\Lambda(\rho \simeq \rho_0) = -30$ MeV [5]. Due to numerical instabilities in calculation of the Brueckner G-matrix, the computation can only be done up to densities $\rho \simeq 3.5\rho_0$. The authors of Ref. [17] then use a quadratic polynomial to extrapolate to higher densities. They calculate the chemical potential for the neutrons and Λs from the Gibbs-Duhem relation using a microscopic EoS computed from a chiral nucleon-meson field theory in combination with functional renormalization group methods. The parameter combinations $(H_1,\ H_2)$ were chosen so that the Λ single-particle potential becomes maximally repulsive at higher densities. The resulting chemical potentials are displayed in Fig. 10 for the NLO19 ΛN forces. These agree well with the HNM(III) chemical potentials up to $\rho \simeq 2.5\rho_0$ but show, different to what we find, no crossing. Note that the forces discussed in [17] have not been applied to finite nuclei.

2B and 3B interaction in AFDMC

For the hyperon sector, we adopted the phenomenological hyperon-nucleon potential that was first introduced by Bodmer, Usmani, and Carlson in a similar fashion to the Argonne and Urbana interactions [44]. It has been employed in several calculations of light hypernuclei [45–51] and, more recently, to study the structure of light and medium mass Λ hypernuclei [34,35]. The two-body ΛN interaction, $v_{\lambda i}$, includes central and spin-spin components and it has been fitted on the available hyperon-nucleon scattering data. A charge symmetry breaking term was introduced in order to describe the energy splitting in the mirror Λ hypernuclei for $A = 4$ [34,47]. The three-body ΛNN force, $v_{\lambda ij}$, includes contributions coming from P- and S-wave 2π exchange plus a phenomenological repulsive term. In this work we have considered two different parametrizations of the ΛNN force.

The authors of Ref. [49] reported a parametrization, hereafter referred to as parametrization (I), that simultaneously reproduces the hyperon separation energy of ${}^{5}_{\Lambda}$He and ${}^{17}_{\Lambda}$O obtained using variational Monte Carlo techniques. In Ref. [34], a diffusion Monte Carlo study of a wide range of Λ hypernuclei up to $A = 91$ has been performed. Within that framework, additional repulsion has been included in order to satisfactorily reproduce the experimental hyperon separation energies. We refer to this model of ΛNN interaction as parametrization (II).

No $\Lambda\Lambda$ potential has been included in the calculation. Its determination is limited by the fact that $\Lambda\Lambda$ scattering data are not available and experimental information about double Λ hypernuclei is scarce. The most advanced theoretical works discussing $\Lambda\Lambda$ force [52,53], show that it is indeed rather weak. Hence, its effect is believed to be negligible for the purpose of this work. Self-bound multi-strange systems have been investigated within the relativistic mean field framework [54–56]. However, hyperons other than Λ have not been taken into account in the present study due to the lack of potential models suitable for quantum Monte Carlo calculations.

Parameterization in AFDMC

$\rho_\Lambda = x\rho$ are the neutron and hyperon densities, respectively. The energy per particle can be written as

$$E_{\mathrm{HNM}}(\rho, x) = [E_{\mathrm{PNM}}((1-x)\rho) + m_n](1-x) + [E_{\mathrm{P\Lambda M}}(x\rho) + m_\Lambda]x + f(\rho, x). \qquad (2)$$

We parametrized the energy of pure lambda matter $E_{\mathrm{P\Lambda M}}$ with the Fermi gas energy of noninteracting Λ particles. Such a formulation is suggested by the fact that in the Hamiltonian of Eq. (1) there is no $\Lambda\Lambda$ potential. The reason for parametrizing the energy per particle of hyperneutron matter as in Eq. (2) lies in the fact that, within AFDMC calculations, $E_{\mathrm{HNM}}(\rho, x)$ can be easily evaluated only for a discrete set of x values. They correspond to a different number of neutrons ($N_n = 66, 54, 38$) and hyperons ($N_\Lambda = 1, 2, 14$) in the simulation box giving momentum closed shells. Hence, the function $f(\rho, x)$ provides an analytical parametrization for the difference between Monte Carlo energies of hyperneutron matter and pure neutron matter in the (ρ, x) domain that we have considered. Corrections for the finite-size effects due to the

EoS(S=-2)

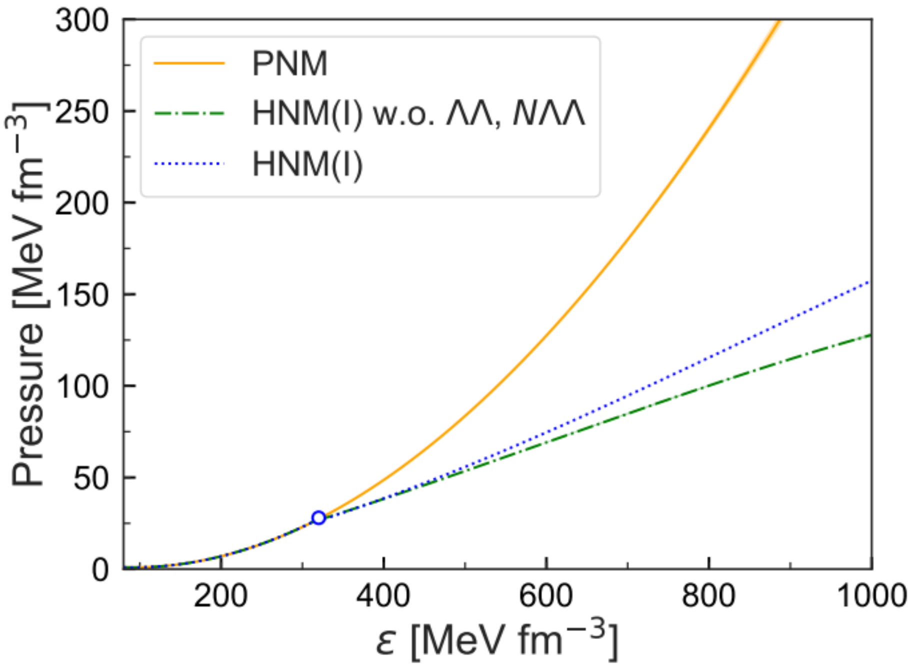

Pressure [MeV fm^{-3}]
ε [MeV fm^{-3}]
PNM
HNM(I) w.o. ΛΛ, NΛΛ
HNM(I)
0
50
100
150
200
250
300
200
400
600
800
1000

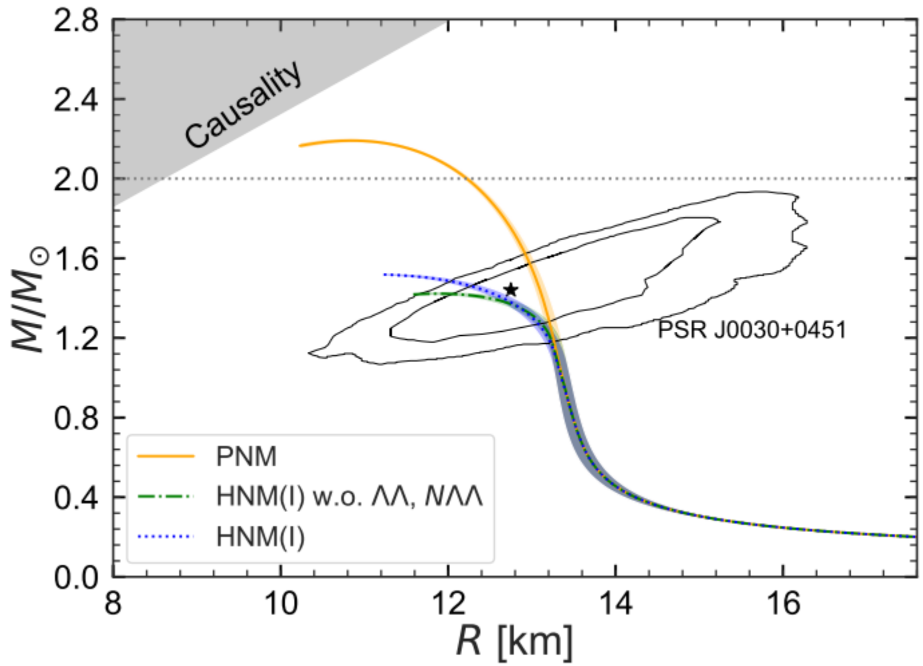

$M/M_\odot$
R [km]
Causality
PSR J0030+0451
PNM
HNM(I) w.o. ΛΛ, NΛΛ
HNM(I)
0.0
0.4
0.8
1.2
1.6
2.0
2.4
2.8
8
10
12
14
16

Many body calculations and NN Interactions

① Density functional theories (DFTs) with effective nucleon–nucleon (NN) interactions

② *ab initio* methods with realistic ones

Realistic Interaction

AV18, CD-Bonn,

χEFT, LQCD…

Many-body method

MBPT, NCSM, CC,

QMC, IM-SRG, BBG,

NLEFT…

✓ EoS with (without) hyperons from NLEFT

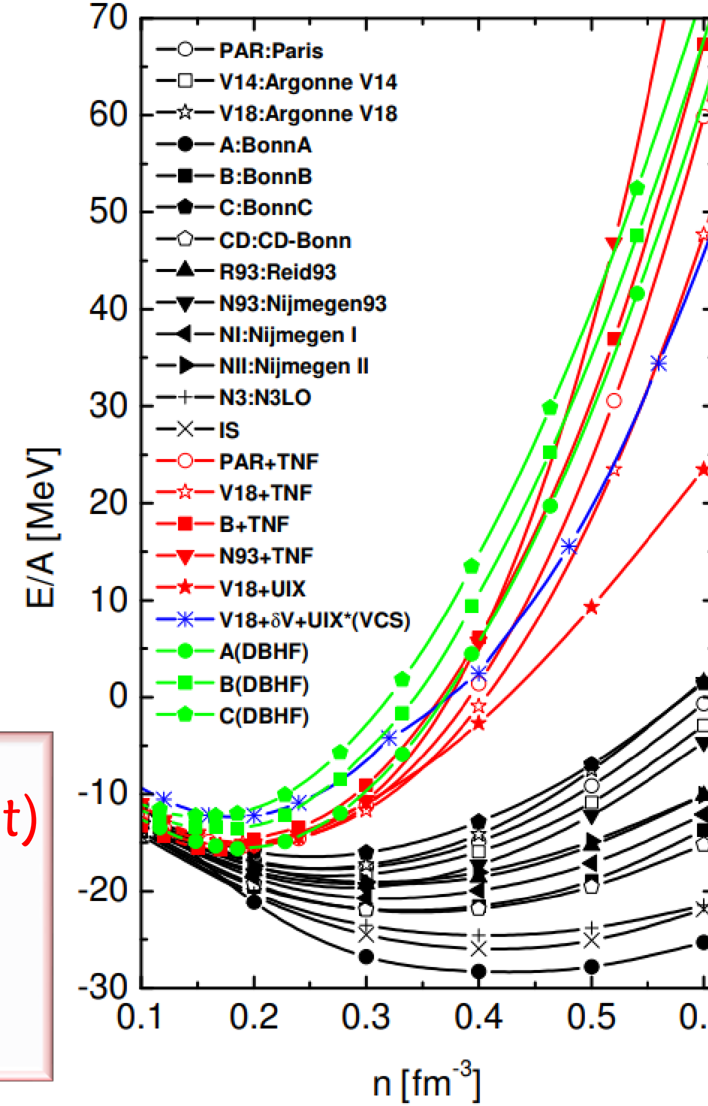

G. F. Burgio, et al., arXiv 1804, 03020 (2018)

From EoS to Neutron Star

- The equation of state (EoS) for dense nuclear matter constitutes the basic input quantity for the theoretical reconstruction of a neutron star.

R. C. Tolman, Phys. Rev. 55, 364 (1939)

J. R. Oppenheimer and G. M. Volkoff, Phys. Rev. 55, 374 (1939)

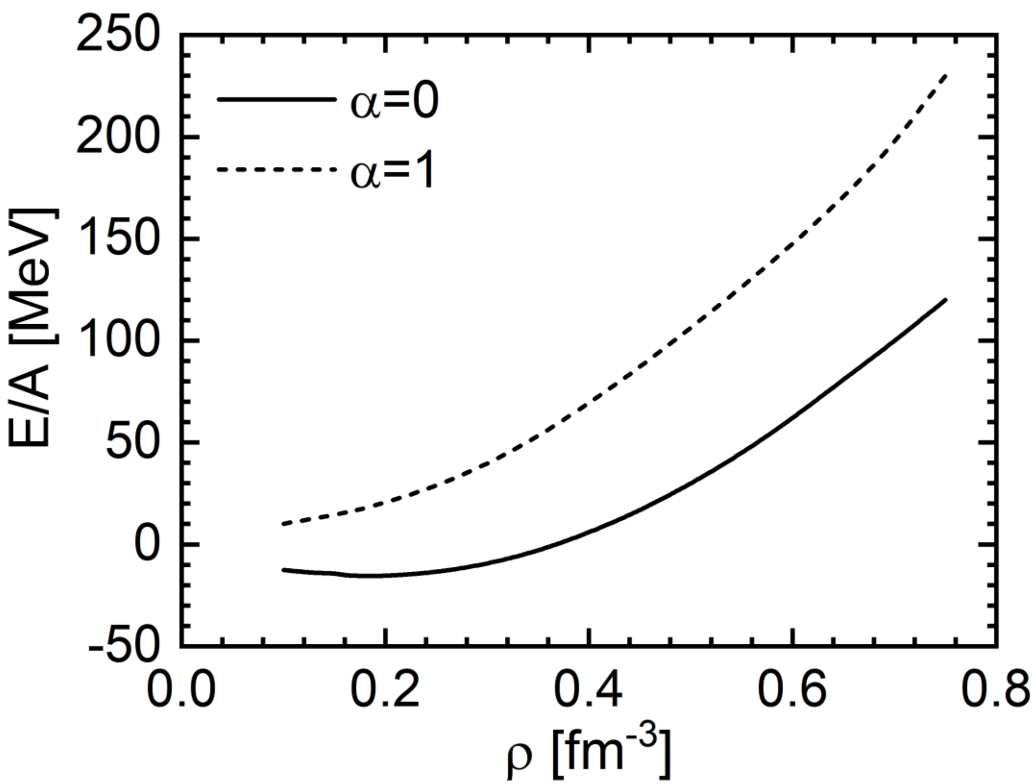

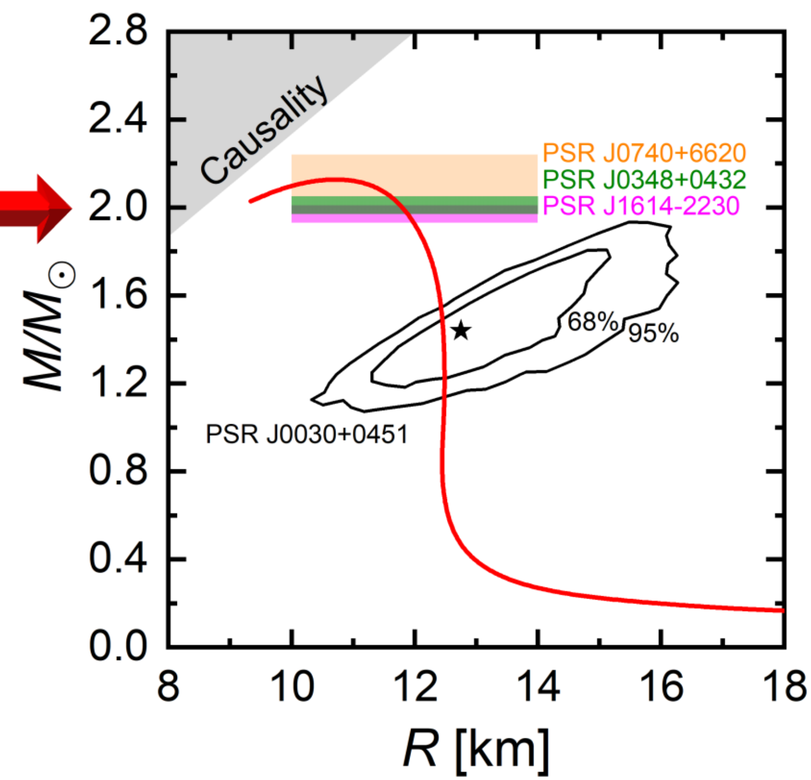

C. H. Lee, et al., Phys. Rev. C 57, 3488 (1998)

Neutron star

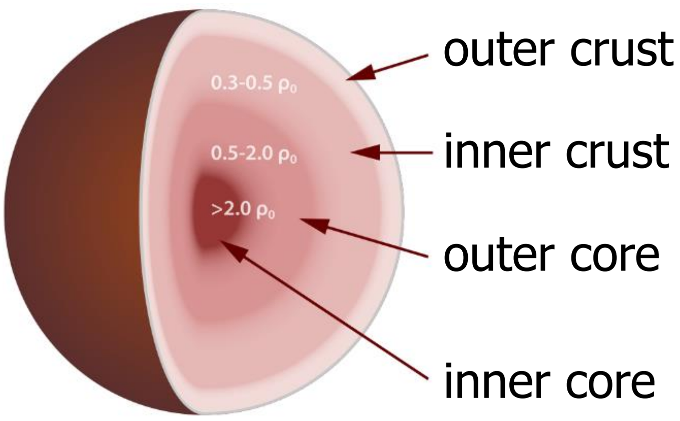

☼ *Figure from www.Universe.com*

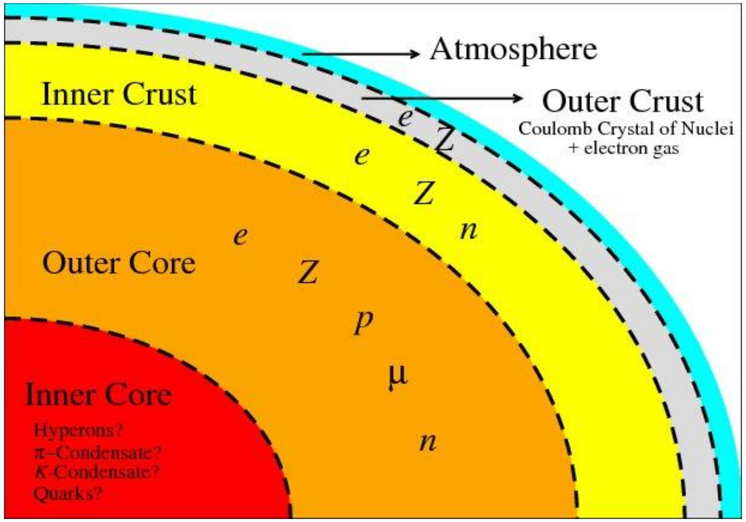

☼ *Figure from J. Piekarewicz*